



Critical assessment of metrics and methods used to quantify temporal loading of rainfall events

Molly Asher^{1,2}, Mark A. Trigg¹, Cathryn E. Birch², Rasmus Henriksen³, Steven J. Böing^{3,4}, and Jonas Wied Pedersen^{3,4}

Correspondence: Molly Asher (gy17m2a@leeds.ac.uk)

Abstract. The distribution of rainfall over a storm's duration, known as the event temporal loading, can significantly influence hydrological and geomorphological responses, including run-off generation, urban flood risk, and soil erosion. A wide range of approaches have been developed to analyse rainfall event temporal loading, but these differ in how they characterise rainfall behaviour and in the aspects of storm structure they emphasise. Early research further suggests that climate change may alter rainfall temporal loading in complex and regionally dependent ways, underlining the importance of clear and consistent approaches to its quantification. In this study, we identify 52 metrics that have been applied to describe event temporal loading, and categorise them as classification metrics, summary statistics, or intermittency metrics. We calculate these metrics for 233,128 rainfall events recorded at Danish rain gauges, and demonstrate that, while some metrics are robust to changes in rainfall event temporal resolution and pre-processing, others are highly sensitive. Data-driven cluster analysis further reveals how various metrics relate to one another, highlighting groups of metrics that may be used interchangeably, and others that describe fundamentally different properties. Based on this, we conceptualise five aspects of temporal loading (mass timing, peak timing, magnitude concentration, temporal concentration, and intermittency) and recommend metrics to quantify each. Overall, the study provides a foundation for more deliberate and informed metric selection, helping to align research questions with appropriate representations of rainfall temporal loading, and offering a clearer basis for cross-study comparison.

15 1 Introduction

Rainfall events vary not only in their total volume and duration but also in how rainfall intensities fluctuate as the storm develops. Storms typically evolve through distinct phases of initiation, intensification, and dissipation, reflecting the dynamic interplay of meteorological and cloud processes. In this study, we use the term 'event temporal loading' to describe this internal variability in intensity over the course of a storm. Similar concepts have been described in the literature under various terms, including the intensity profile (Dunkerley, 2021a), storm profile (Kottegoda and Kassim, 1991), rainfall temporal pattern (Wang, 2020), and intra-event rainfall variability (Todisco, 2014).

¹School of Civil Engineering, University of Leeds, Leeds, UK

²Institute for Climate and Atmospheric Science, University of Leeds, Leeds, UK

³Weather research, Danish Meteorological Institute. Sankt Kjelds Plads 11, 2100 Copenhagen O, Denmark.

⁴DTU Sustain, Technical University of Denmark. Bygningstorvet Building 115, 2800 Kgs. Lyngby, Denmark



30

50



Rainfall event temporal loading has been shown to influence hydrological and geomorphological responses across a wide range of environmental processes, however the direction and magnitude of its effects often vary between studies. For instance, flood modelling experiments have demonstrated that temporal loading alone can produce flood depth differences of up to 35% under identical rainfall volumes (Hettiarachchi et al., 2018). In landslide studies, early-peaking storms have been associated with greater infiltration and more severe slope instability (Fan et al., 2020). Soil erosion studies exemplify the diverging outcomes in temporal loading studies. Wang et al. (2016) reported greater soil loss from later-peaking storms, while Aquino et al. (2013) found early-peaking events to be more damaging. Such differences underscore that while temporal loading is clearly influential, its specific impacts depend on system characteristics, dominant processes, and methodological approaches. Extreme rainfall events are expected to intensify in a warming climate at around 6–7% per degree Celsius, following the Clausius–Clapeyron (CC) relationship (Trenberth et al., 2003). Furthermore, for short-duration convective extremes, some studies suggest even greater rates of intensification, known as super-CC scaling (Fowler et al., 2021). This behaviour has been likely to develop a superior of the process and accuration can be a superior of the process and a convective call develop.

Clausius–Clapeyron (CC) relationship (Trenberth et al., 2003). Furthermore, for short-duration convective extremes, some studies suggest even greater rates of intensification, known as super-CC scaling (Fowler et al., 2021). This behaviour has been linked to dynamical storm changes under higher temperatures, including variations in storm speed, convective cell development, and feedbacks such as latent heat release (Lenderink and Van Meijgaard, 2009; Fowler et al., 2021). These dynamical storm processes have also been suggested to affect the temporal distribution of rainfall within storms. A growing body of work has begun to examine how event temporal loading may change in a warmer climate (Visser et al., 2023; Ghanghas et al., 2024; Asher et al., in press; Wasko and Sharma, 2015), but results to date show variable magnitudes and directions of change, pointing to possible regional dependencies in behaviour. Research in this area remains at an early stage and is developing actively.

Despite its demonstrated importance, rainfall event temporal loading is often oversimplified or overlooked in impact modelling applications. While high-resolution data (e.g., 1–5 minutes) are ideal for capturing the short, intense bursts of rainfall critical for urban hydrology (Schilling, 1991; Einfalt et al., 2004; Berne and Krajewski, 2013), in reality many observational precipitation datasets are provided at lower resolutions. Rainfall impact modelling studies also frequently rely on derived or synthetic events. Here idealised or averaged storm profiles tend to prioritise capturing total volume and duration, at the expense of sub-event dynamics such as peak intensity timing or concentration. For example, symmetrical, centrally peaked intensity profiles are commonly used in flood modelling, such as the FEH design profiles in the UK (Centre for Ecology & Hydrology, 1999) and the Chicago design storm used in the US and other countries (Keifer and Chu, 1957). As a result, the full range of possible hydrological responses may not be represented, leading to underestimation of peak flows, misrepresentation of drainage performance, and failure to identify critical scenarios, compromising risk assessments, infrastructure design, and climate adaptation planning.

Robust, interpretable metrics are therefore essential to bridge the gap between observed rainfall behaviour and the simplified forms commonly used in models. By quantifying key aspects of temporal loading, such metrics help preserve important features when rainfall events are simplified, improving the fidelity of hydrological representations. Furthermore, metrics can offer insight into why the influence of temporal loading varies across studies and contexts, by revealing which specific aspects of storm evolution are most relevant to particular hydrological responses. A wide variety of metrics have been proposed and used to describe event temporal loading. However, there has been little systematic evaluation of how these metrics relate to one another, how sensitive they are to temporal resolution and data processing choices, or whether they are broadly suitable across





hydrological and climatological contexts. There is also a lack of clear terminology: metrics often target different characteristics, such as asymmetry, peakiness, or intermittency, but these distinctions are not always explicit. The relevance of each aspect varies by discipline, and borrowing metrics across domains can result in misplaced emphasis or misinterpretation.

This study seeks to address gaps in knowledge on how temporal loading metrics perform under different data and processing conditions, and on how metrics relate to one another. The work addresses the following research questions:

- RQ1: What key properties of rainfall event temporal loading are commonly measured, and why?
- RQ2: How sensitive are these metrics to the temporal resolution of the rainfall data?
- RQ3: How does de-dimensionalisation of rainfall events affect metric values?
- RQ4: Which metrics are strongly correlated, suggesting they may be redundant or are suitable for use in cross-comparison of studies.

The first research question is addressed through a structured review that identifies existing metrics used to quantify temporal loading, followed by a synthesis of their underlying assumptions, intended applications, and data requirements (Sect. 2). The remaining questions apply data from Danish rain gauges. The second and third questions are examined via comparative analyses of metrics calculated on rainfall events at varying temporal resolutions (Sect. 4.1) and with normalisation applied (Sect. 4.2). Finally, the last research question is tackled using cluster analysis to explore similarities among metrics calculated from raw rainfall events at a 5-minute resolution (Sect. 4.3).

2 Literature review

2.1 Search and selection strategy

The literature review follows the PRISMA (Preferred Reporting Items for Systematic Reviews and Meta-Analyses) framework (Moher et al., 2010). The PRISMA framework is a standardised method of performing literature review which aims to minimise potential researcher bias, and to promote transparency and reproducibility in the identification and selection of relevant studies. The framework includes four key stages: (1) identification, boolean queries used to identify potential studies, duplicated studies removed; (2) screening, abstract level review to remove irrelevant studies; (3) eligibility, full-text review against pre-defined inclusion/exclusion criteria; and (4) inclusion, relevant studies included for review, and the total number of studies reported.

Boolean queries are search strings using AND, OR and NOT operators, and are constructed here by combining different terms used in the literature to describe event temporal loading, with different terms used to describe rainfall events. The full queries used to search the Scopus, Web of Science, and Google Scholar databases are outlined in Appendix A. The searches were performed on the 15/02/2025 and returned 903 relevant records overall (including 181 on Scopus, 409 on Web of Science, and 313 on Google Scholar). 351 duplicated records were removed, leaving 552 studies for abstract level screening. After screening of abstracts, a further 390 studies were eliminated, leaving 162 papers for full review.



100

105

110

120



Studies were included if they met the following criteria: (a) use of search terms in the title, abstract, or keywords; (b) published in English; (c) focus on individual rainfall events with data at sub-daily temporal resolution; (d) application of a method or metric to quantify temporal loading. Exclusion criteria were: (a) not published in English; (b) inaccessible or behind paywalls (to the authors, not all included studies are open-access); (c) lack of use of sub-daily rainfall data; (d) combined spatial and temporal analysis (where the temporal loading could not be separated); (e) focus on rainfall trends over extended periods (e.g., seasonal or monthly scales); (f) no application of a metric for quantifying within-event temporal variability.

After applying these criteria, a total of 59 studies remained. We note, however, that several additional studies met all criteria except the use of a metric to quantify temporal loading. These excluded studies fall into three main groups. The first concerns the disaggregation of daily rainfall data (Pampaloni et al., 2021). The second includes stochastic event generation approaches (Cha et al., 2024; Efstratiadis et al., 2022; Kao and Govindaraju, 2008; Nguyen and Chen, 2022; Oriani et al., 2018; Pampaloni et al., 2021). The third involves applications of synthetic rainfall events with prescribed temporal patterns to investigate impacts on soil erosion (De Lima and Singh, 2002; de Lima et al., 2013; Frauenfeld and Truman, 2004; Gao et al., 2018; Parsons and Stone, 2006; Wang et al., 2023), landslides (Zhao et al., 2025), and herbicide runoff (Zhang et al., 1997). In these cases, event profiles are described using broad qualitative labels (e.g. linearly increasing, stepped increasing–decreasing, uniform) rather than being quantified with explicit metrics.

2.2 Domains and purposes of reviewed literature

Research on rainfall temporal loading spans a range of domains concerned with hydrological and geomorphological responses to precipitation. The most prominent domain is flood modelling, where studies range from rainfall-runoff models in large watersheds (Cai et al., 2024), to the hydraulic performance of urban sewer systems (Li et al., 2021; Müller et al., 2017). Other domains include soil erosion and sediment transport (Römkens et al., 2002; Liu et al., 2022; Dunkerley, 2021a; Rivera et al., 2012; Gao et al., 2024; Wang et al., 2016; Alavinia et al., 2019; Gholami et al., 2021; Aquino et al., 2013; Klamkowski et al., 2012), pollution modelling (Fu et al., 2021), rainfall-induced landslides (Fan et al., 2020), and climate change impact assessments on extreme rainfall characteristics (Visser et al., 2023; Hu et al., 2018).

Despite the range of contexts, research is generally motivated by similar questions. One common aim is to assess system sensitivity to rainfall temporal loading. This is typically performed by running models with rainfall events of fixed total volume and duration but varying temporal distributions, before examining the resulting impacts on, for example, peak flow, runoff volume, or pollutant wash-off (e.g. Asher et al. (2025)). While these studies treat the system as the subject of analysis (i.e., asking how sensitive a model or process is to rainfall structure), others assume system sensitivity and focus directly on the characterisation of rainfall events themselves. This includes research developing new or more nuanced metrics for describing internal rainfall variability (Todisco, 2014; Dunkerley, 2022), or research applying existing metrics to group and summarise events into representative hyetographs for specific locations, e.g., for China by Wang (2020), Iran by Amin et al. (2000), Slovenia by Dolšak et al. (2016), Greece by Vantas et al. (2019), amongst numerous others. Such work is often intended to improve development of design storms or evaluate how well standard hyetographs reflect observed temporal patterns. Finally, in stochastic rainfall generation and disaggregation, metrics help ensure that synthetic rainfall sequences reproduce realistic intra-





event patterns, preserving statistical characteristics critical for sub-daily modelling. Across all these purposes, the consistent goal is to represent temporal loading more accurately in a way that enhances understanding, modelling performance, and decision-making.

The reviewed studies rely on two main sources of rainfall data: observational records or synthetically generated events. The majority of studies use events extracted from observed rainfall time series, typically recorded by rain gauges, e.g., Zhang et al. (2023), or radar, e.g., Urgilés et al. (2024). Events are extracted from observational records based on assumptions about what constitutes the start and end of a rainfall event, such as minimum intensity thresholds or inter-event dry periods (Restrepo-Posada and Eagleson, 1982). However, event boundaries and characteristics are inevitably shaped by the temporal resolution of the observational dataset, and so 'observed' rainfall events remain approximations shaped by the resolution of the measurement system, rather than exact representations of storm behaviour.

Other studies on event temporal loading use synthetic rainfall events, generated for controlled experimentation or scenario testing (e.g., Cai et al. (2024), Bezak et al. (2018), Fan et al. (2020)). These synthetic events typically fall into two broad categories: idealised design storms and stochastically generated events. Idealised storms take simple geometric forms, such as uniform rainfall, or triangular profiles peaking early, centrally, or late (e.g., Parsons and Stone, 2006), and are used to systematically explore the influence of temporal loading while abstracting from site-specific variability. These types of events are used in the studies noted in Section 2.1 but not included in our review as they do not quantify event temporal loading with a metric. In these studies, the idealised profiles often form the basis for physical experiments, where pre-defined rainfall patterns are applied to laboratory set-ups simulating hillslopes or infiltration systems (Wang et al., 2023; de Lima et al., 2013; Parsons and Stone, 2006; Zhang et al., 1997). In contrast, stochastically generated events, produced using rainfall generators, aim to replicate the statistical properties of observed rainfall while allowing control over event magnitude and duration. The synthetic events are typically applied within modelling frameworks to explore a broader range of possible rainfall scenarios. While use of synthetic rainfall enables controlled investigation of temporal effects, it necessarily involves assumptions about what constitutes a "representative" event. These assumptions can affect the interpretation of results, particularly when attempting to generalise findings to real-world conditions.

145 2.3 Rainfall processing choices

150

Research varies not only in the type of rainfall data used, but also in how that data is processed before applying temporal loading metrics. In some studies, metrics are applied directly to the raw rainfall intensity series. This retains the original units and absolute values of the event, allowing metrics to reflect both timing and intensity. In contrast, other studies use double normalised representations, known as dimensionless mass curves (DMCs) or Huff curves (Huff, 1967), in which both cumulative rainfall and event duration are scaled between 0% and 100%. Interpolation is often applied at regular intervals (e.g., every 1% or 10% of the storm duration) to enable comparison between events.

Normalised representations are widely used in studies seeking to generalise across events or derive representative storm profiles. By removing differences in scale and duration, DMCs allow researchers to isolate temporal loading and compare the shapes of events more directly across events of different magnitude and durations. In some cases, mean DMCs are computed



160

170

175

180

185



for specific regions by averaging across many events (see Sect. 2.2). These regional profiles are used to justify the use of particular design storms or to critique existing design standards. Other studies use DMCs as a basis for classifying events, for instance Huff curves are typically labelled according to the quartile of the Huff curve containing the most rainfall.

Despite the widespread use of DMCs, the effects of normalisation on metric outcomes are often not clearly articulated. Some studies report metrics calculated on both raw and normalised data, but many do not specify the format used at all. This lack of transparency complicates comparisons across studies and makes it difficult to assess whether observed patterns reflect intrinsic features of the events or artefacts of data processing.

2.4 Typology of metrics

The wide range of metrics identified in the reviewed studies are listed in Tables C1, C2 and C3 in Appendix C. Based on our own conceptual understanding of the metrics, and their description in the literature, we have assigned each of them to one of three metric types: classification metrics, summary statistics, and intermittency metrics. The categories and how they are delineated is described below.

2.4.1 Classification metrics

Classification metrics assign discrete labels to rainfall events. A common approach categorises events by the fraction of the storm that contains the most significant portion of rainfall, typically a third (Horner and Jens, 1942; Aquino et al., 2013; Wang et al., 2016; de Assunção Montenegro et al., 2018; de Andrade et al., 2020), quarter (Huff, 1967; Amin et al., 2000; Jun et al., 2021; Harshanth et al., 2023; Azli and Rao, 2010; Amponsah et al., 2019; Wartalska and Kotowski, 2020; Vantas et al., 2019; Loukas and Quick, 1996; Dolšak et al., 2016; Li et al., 2021; Bezak et al., 2018), or fifth (Villalobos Herrera et al., 2023; Ng et al., 2001; Asher et al., 2025). While simple, the outcomes of such classifications depend heavily on implementation choices. For example, Horner and Jens (1942) introduced the original third-based classification scheme, defining events as advanced, intermediate, or delayed based on the timing of the peak. By contrast, Liang et al. (2023) also use thirds but classify events based on the location of the rainfall mass, identifying the third with the highest total rainfall. Further refinements to this method classify events based on the third containing a summary statistic, e.g. the centre of gravity or D₅₀ (see Sect. 2.4.2). Figure 1 provides an illustrative example of some classification metrics.

More complex classification schemes compare the dimensionless mass curve of an event to that of a uniform storm. For instance, Terranova and Iaquinta (2011) assign a four-digit Binary Shape Code (BSC) based on whether cumulative rainfall in each quartile exceeds that of a uniform distribution. Kottegoda and Kassim (1991) use the crossing properties concept to classify events with a number based on the number of times the event DMC crosses the uniform DMC, and a letter, which describes whether it exhibits a generally increasing or decreasing intensity profile.

Overall, classification metrics simplify complex event structures into interpretable categories, and provide a tractable way to group storms by structural type. This is particularly useful in design and modelling contexts, where efficiency and consistent processes are important. However, their categorical nature may mask finer differences between events and may be sensitive to how the storm duration is divided.





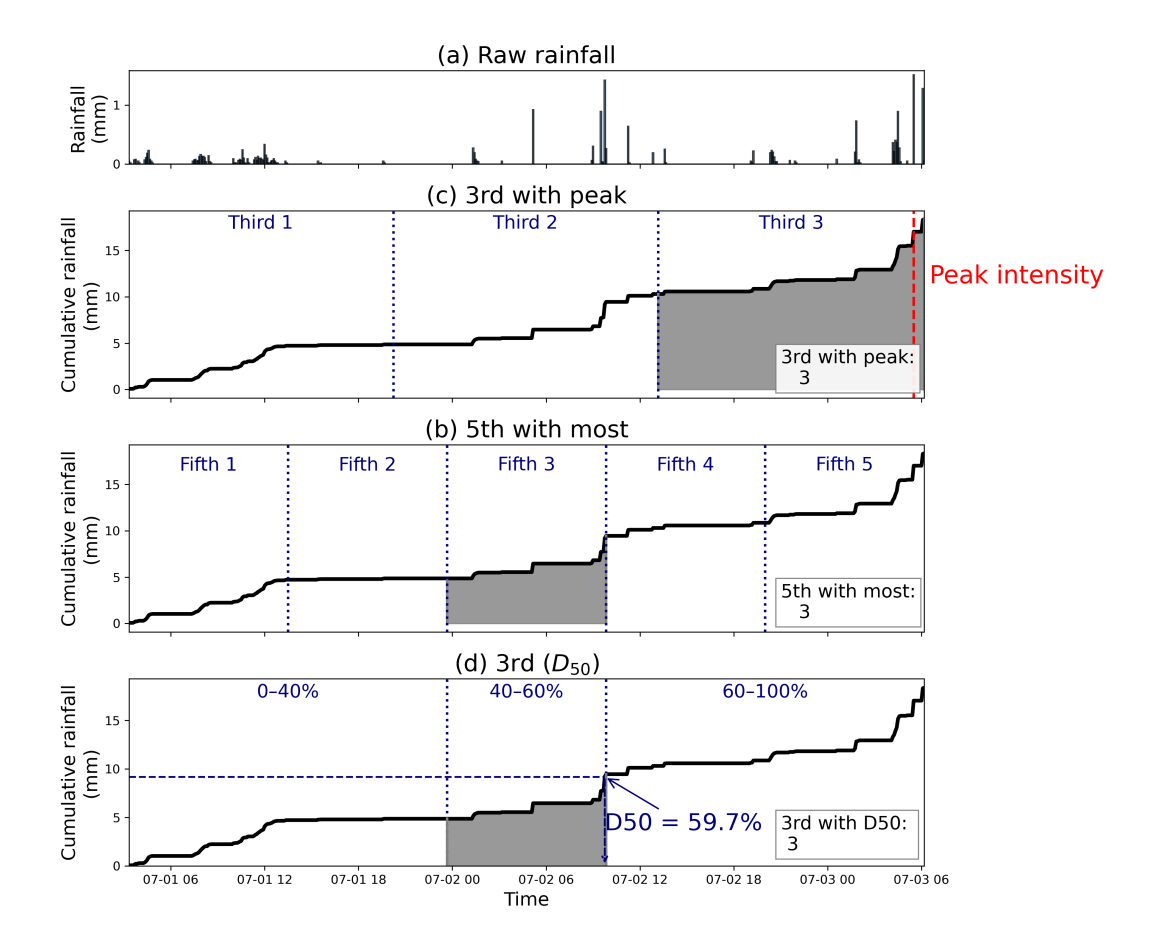


Figure 1. Illustration of some classification metrics for an example rainfall event: (a) the raw rainfall data, and classification of the event based on (b) 3rd with peak (Aquino et al., 2013; Fatone et al., 2021; Pinheiro et al., 2018; Wang et al., 2016), (c) 5th with most rainfall (Villalobos Herrera et al., 2023), (d) 3rd with D_{50} (Visser et al., 2023).

2.4.2 Summary statistics

190

195

Summary statistics are continuous metrics that quantify variation in rainfall intensity over time. We broadly group them into three types based on the way they are described in the literature: **peakiness indicators**, **asymmetry indicators**, and **concentration indicators**.

Peakiness indicators capture how sharp or pronounced the intensity of peaks are relative to the rest of the storm. Metrics such as *maximum intensity*, *mean intensity*, and *I30* (the maximum rainfall depth accumulated in any 30-minute period) provide baseline measures of peak magnitude and concentration. Other common examples include the *standard deviation*, *coefficient of variation*, *classical skewness*, and *classical kurtosis*, borrowed from general statistics, which reflect variability and the prominence of extremes across the distribution (Brommer et al., 2013; Yang et al., 2015; Kimura et al., 2014; García-Bartual



200

205



and Andrés-Doménech, 2017; He et al., 2024). A number of metrics specifically compare the peak with the mean. These include the *peak-to-mean ratio* (also called the rainfall intensity irregularity (Wartalska et al., 2020)), and the *relative amplitude*, defined as the range divided by the mean (Gao et al., 2024; Liu et al., 2022). As the minimum intensity is often 0 mm/hr, and otherwise very close to 0, these two metrics are often equivalent. Similarly, *m2* compares the amount of rainfall in the highest intensity time step to the total event volume (Wartalska et al., 2020), while zone-based metrics, such as the *mean intensity within HIZ* (periods exceeding the event average), quantify how extreme the most active parts of the storm are relative to the overall distribution (Liu et al., 2022).

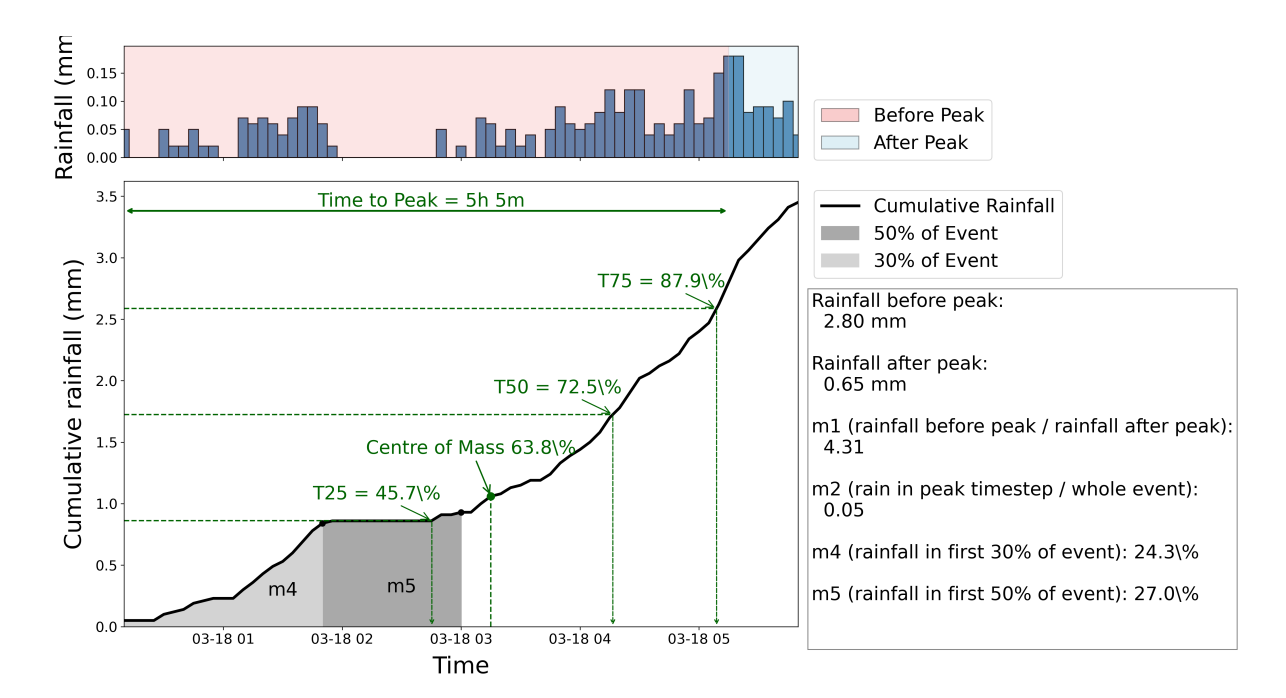


Figure 2. Illustration of several summary statistics for an example rainfall event, including *m1*, *m2*, *m4*, *m5* (Wartalska and Kotowski, 2020), *T25*, *T50*, *T75* (Knighton and Walter, 2016), *centre of mass* and *time to peak* (Jun et al., 2021; Knighton and Walter, 2016)

Lateral asymmetry indicators quantify whether rainfall is concentrated toward the beginning or end of an event. As with classification metrics, some indicators focus on the timing of peak intensity, while others describe the distribution of the rainfall mass across the event duration. Metrics such as *time-to-peak* and the *peak-position-ratio* (also called the coefficient of peak rainfall intensity) describe how early or late the maximum intensity occurs (Fu et al., 2021; Wartalska and Kotowski, 2020; Cai et al., 2024; Wartalska et al., 2020; Knighton and Walter, 2016). *Skew_p* is also anchored to the peak timing, but measures the relative position of the peak within the rainfall duration (Oh et al., 2024). Other metrics capture asymmetry across the entire rainfall mass. The *m1* metric compares the volume of rainfall before versus after the peak (Wartalska et al., 2020), while the *event loading index* similarly contrasts pre- and post-peak rainfall (Ghanghas et al., 2024). Percentile timing indicators such as the *centre of gravity*, *D*₅₀ (Visser et al., 2023), and *T25%*, *T50%*, and *T75%* (Knighton and Walter, 2016) describe how



220

225

230

235

240



rainfall accumulates over time. Müller et al. (2017) introduce *asymmetry of dependence* to describe the degree to which an event timeseries is reversible. Mass distribution indicators *m3*–*m5* express the proportion of rainfall in the first 33%, 30%, and 50% of the event duration (Wartalska et al., 2020), while Liu et al. (2022) calculate the proportion of rainfall in each quarter of the event (*fraction Q1*, etc). A number of these asymmetry based metrics are visualised in Figure 2.

Concentration indicators describe how rainfall is clustered within an event. A key example is the *Precipitation Concentration Index (PCI)*, originally developed to assess monthly and seasonal rainfall distributions (Oliver, 1980) but also applied to individual events (He et al., 2022). Higher *PCI* values indicate a greater share of rainfall concentrated in fewer time steps. The *Temporal Concentration Index (TCI)* was introduced as a scale-independent alternative that could be used to compare across events of different durations (Long et al., 2021). It quantifies the deviation of an event's temporal loading from that of a uniform rainfall event with the same duration and volume. Another related measure is the normalised root-mean-square error around the peak (*NRMSE_p*), which assesses how tightly rainfall is clustered near the peak time step (Oh et al., 2024). The *Gini coefficient*, originally developed to measure income inequality, has also been adapted to assess the unevenness of rainfall distribution within an event (Lu et al., 2025). Applied to rainfall, it reflects how much cumulative rainfall deviates from a perfectly even distribution. For highly concentrated events, the accompanying *Lorenz asymmetry coefficient* describes whether this arises from a few extreme high-intensity bursts or from many moderately intense intervals, both of which could lead to high concentration. Zone based indicators, including the % *of rainfall in high-intensity zone (HIZ)*, *time in high-intensity zone (HIZ)/low-intensity zone (LIZ)*, indicate how long the storms stays intense and how much rainfall is concentrated in these intense bursts (Liu et al., 2022).

2.4.3 Intermittency metrics

Intermittency metrics are designed to capture the presence and frequency of dry periods within rainfall events. These metrics are particularly relevant in contexts where wet–dry fluctuations affect hydrological processes such as infiltration, soil saturation, and flash flood generation. Although fewer in number than other metric types, intermittency measures add an important dimension to the characterisation of temporal loading by highlighting fluctuations that may not be captured by peak-based or cumulative statistics. The *event-dry ratio* calculates the proportion of time steps within an event that record no rainfall as a proportion of the total number of recorded intervals in the event (Pohle et al., 2018). Relatedly, the *intermittency fraction* measures the number of transitions from wet to dry during the event, giving a more specific idea of whether event rainfall is very disparate (Dunkerley, 2021b).

2.5 Metrics summary

Sects. 2.2–2.4 review the selected studies in terms of their objectives, the types of metrics employed, the rainfall data sources used, and the processing steps applied. The distribution of these characteristics across the reviewed studies is summarised in Table 1, while a full overview of all studies is provided in Table B1 in Appendix B.

Figure 3 presents the number of studies applying each metric and highlights the geographical focus of those studies. The figure shows that most metrics have only been applied in one or two papers, with a small number dominating the literature.





Table 1. Summary of studies by purpose, metric type, the type of rainfall events used in the study, and the processing stages applied. Note that some studies may be counted under more than one categorisation

Category	Subcategory	Detail	Number of studies
	Characterise rainfall profiles in an area	23	
		Flooding/hydrology	12
		Landslide	1
Study purpose	Impact of storm temporal profile on:	Pollution	2
		Soil erosion	13
	Climatic study		5
	Stochastic event generation		3
	Evaluating satellite data		1
	Metric development		4
N/14** 4	Classification		33
Metric type	Summary stats		25
	Intermittency		2
D - 1 - 6 - 11 4	Real		47
Rainfall type	Synthetic		12
) a i u f a 11 a a a a i a a	Raw rainfall events		24
Rainfall processing	Dimensionless Mass Curves		28
	Unclear		7

Classification metrics, which have been in use for several decades, are the most prevalent. Among these, two interpretations of Huff quartiles, the *4th with most* and *4th with peak*, first introduced in 1967, have been applied extensively across different regions. The *3rd with peak*, derived from the earlier work of Horner and Jens (1947), is also frequently used, with a particular concentration of studies focusing on soil erosivity in Brazil.

250 3 Methods

255

3.1 Rainfall data

This research uses rainfall events extracted from Danish rain gauge data at 1 minute resolution. Figure 4 shows the national Danish rain gauge network, which is maintained and operated by the Danish Meteorological Institute (DMI). The individual gauges in the network are mainly owned by DMI and the Danish water utilities organised through the 'Water Pollution Committee of The Society of Danish Engineers' (abbreviated 'SVK" in Danish for 'Spildevandskomiteen'). DMI's gauges are



260

265

270



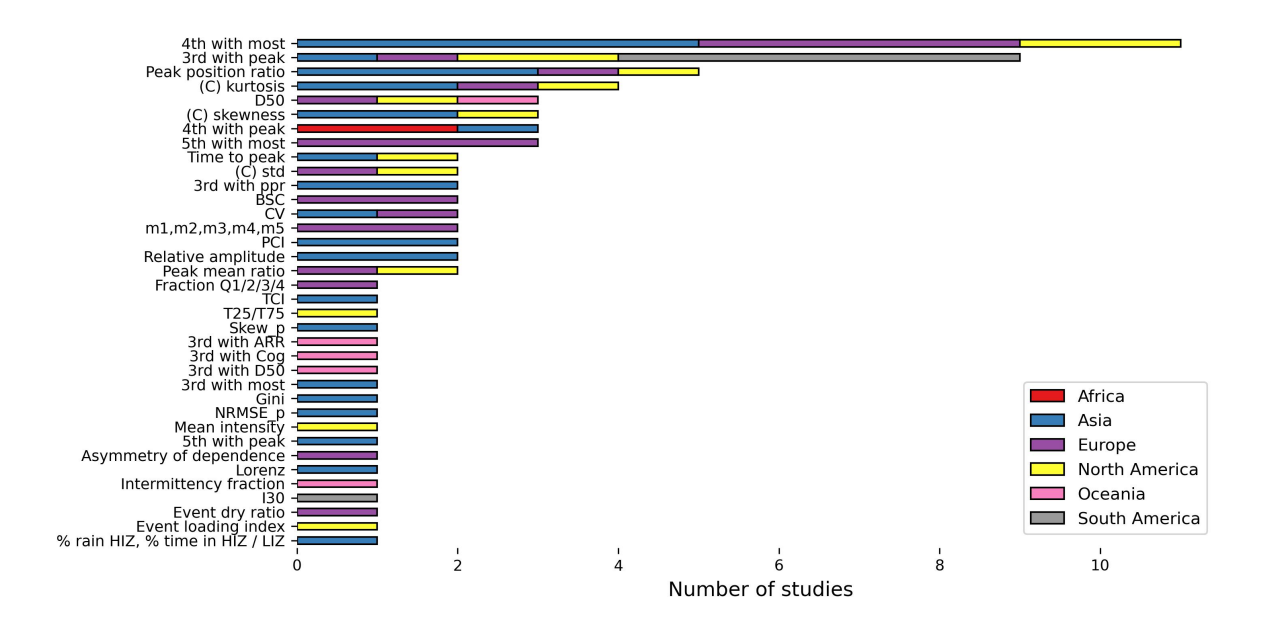


Figure 3. Distribution of metrics across the reviewed studies, showing both the number of studies in which each metric was applied and the countries from which these studies were drawn.

weighing rain gauges of the brands Geonor and OTT Pluvio². The measurement resolution of Geonor gauges are 0.1 mm, while the resolution of the Pluvio² gauges started at 0.1 and was updated during the time period focused on in this study to 0.01 mm. SVK's gauges are tipping bucket gauges by Rimco with a measurement resolution of 0.2 mm. Both gauge types record data with a temporal resolution of one minute. Figure 4 (left) shows that all DMI's gauges have been operational for less than 15 years, while there is a much larger spread in time series lengths for the SVK gauges with the oldest ones providing continuous time series from 1979 to the present. Figure 4 (right) shows the spatial locations of the gauges with DMI gauges being relatively evenly spread across the country, while SVK gauges cluster around the major cities.

Data quality control for all gauges in the network are performed manually by DMI's climatology department (DMI, 2025). Data points ruled non-trustworthy by manual quality control are excluded from this study.

3.2 Rainfall event extraction and pre-processing

For each rain gauge, independent rainfall events are extracted over the full period of available data. The rainfall time series is first aggregated to 5-minute resolution. This resolution is deemed to best preserve temporal detail, while minimising noise due to the measurement resolution of the rain gauge data. This noise arises because both tipping-bucket gauges and weighing gauges record rainfall in discrete increments, when the buckets tip or when the accumulated weight flips a decimal, which leads to many small, artificial peaks in the 1-minute time series. To ensure event independence, we extract events using a minimum interevent time (MIT) threshold (Restrepo-Posada and Eagleson, 1982; Molina-Sanchis et al., 2016). An 'event' thus constitutes



275

280



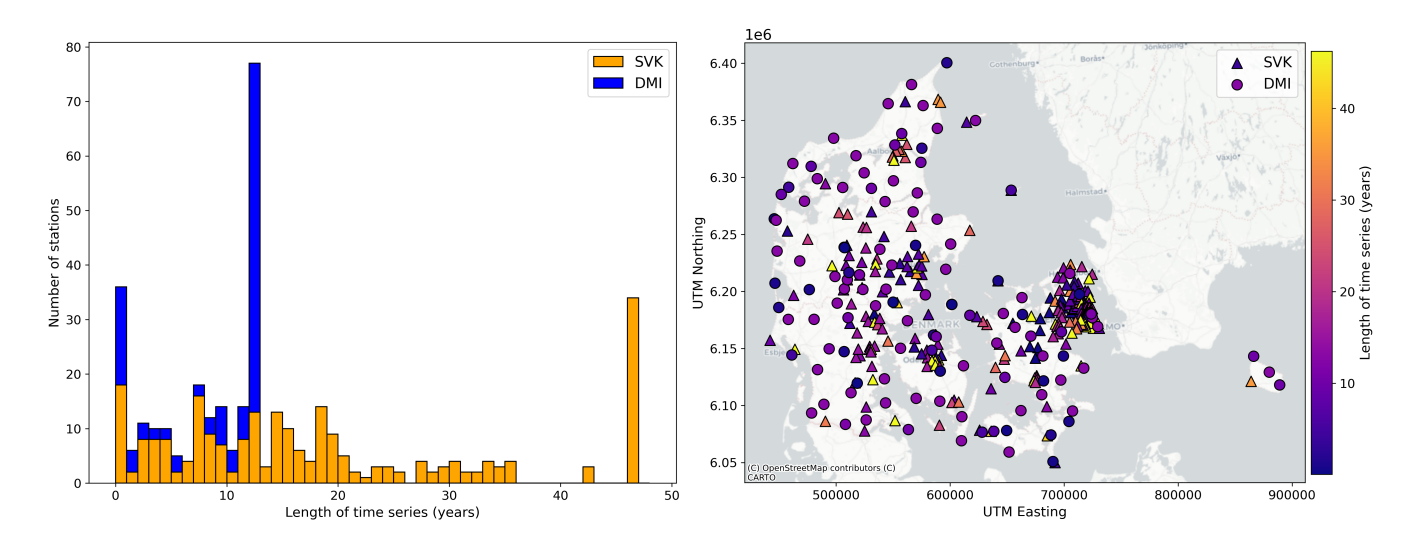


Figure 4. A stacked histogram of the length of the time series for rain gauges (left), and a map of Denmark showing the locations of each gauge, including indications of gauge ownership and time series length (right). Base map: © OpenStreetMap contributors 2025. Distributed under the Open Data Commons Open Database License (ODbL) v1.0.

any rainfall separated by at least 11 hours of rain-free conditions, following practice in several Danish hydrological studies (Gregersen et al., 2013; Thomassen et al., 2023). This approach ensures that each event begins and ends with non-zero rainfall. The MIT parameter has been shown to play an important role in determining the number and properties of rainfall events selected (Dunkerley, 2008). For temporal loading, which is interested in what happens around the peak, the way in which the edges of the event are defined is particularly important, but in this research we do not investigate its influence further.

We define and analyse entire rainfall events, rather than only the most intense 'burst' periods, capturing the complete temporal evolution of each storm. Events with less than 4 mm of total rainfall are excluded to remove very light events unlikely to be hydrologically significant. This process produces a dataset of 233,128 rainfall events observed between 1979 and 2025.

Coarser-resolution versions of each event are also derived at 10-, 30-, and 60-minute resolutions. These are generated based on the start and end times of the 5-minute event, so for a given coarser resolution, the first timestamp equal to or before the 5-minute event start is taken as the new start, and the last timestamp equal to or later than the event end is taken as the new end. As a result, the duration of events at coarser resolutions may be equal or longer in the duration than their 5-minute counterparts.

3.3 Dimensionless mass curve generation

Dimensionless mass curves (DMCs) are generated from all 5-minute resolution rainfall events. A DMC represents the cumulative distribution of rainfall within an event, scaled such that both time and accumulated rainfall range from 0% to 100%. Each DMC is interpolated to have 10 equally spaced time points. Importantly, while DMCs are typically defined as cumulative profiles, in this analysis we derive a double normalised incremental representation by converting each interpolated DMC back into incremental rainfall. This version reflects rainfall intensity as a proportion of total event mass, distributed over relative time.



300

305

315

320



All temporal loading metrics in this study are applied to these 10-point, double normalised incremental series rather than to cumulative curves. This preserves consistency with how metrics are typically applied to raw rainfall intensities, while enabling direct comparison across events in a dimensionless domain.

3.4 Metric computation and post-processing

Rainfall temporal loading metrics are implemented in Python based on the definitions provided in the original publications. In some cases, the literature lacks sufficient detail on the precise application of metrics (e.g., with respect to temporal resolution, handling of zero values, normalisation procedures). Where ambiguity exists, we make reasonable interpretations of the provided formulations. Two of the identified metrics - the Binary Shape Code and the event's Crossing Properties - are not straightforward numeric indicators and are thus deemed outwith the scope of this study.

In addition to the literature-identified metrics, we compute a set of statistical moments on each event's intensity profile to help interpret our clustering results. These include classical moments, which are calculated on the raw sequence of intensities without respect to their temporal order. These include the *classical mean*, which is the mathematical average of the intensity values; the *classical standard deviation*, which is the root-mean-square deviation of intensities from their mean, i.e. the typical spread or variability of rainfall rates (previously applied to rainfall events by García-Bartual and Andrés-Doménech (2017)); the *classical skewness*, which measures the asymmetry of the intensity distribution around the *classical mean*; and the *classical kurtosis*, which measures tail-heaviness or peakiness of the intensity distribution around that centre.

We also calculate temporal moments which consider the distribution of intensity values in respect to time. These include the *temporal mean* (referred to here as the *centre of gravity*), which weights each time step by its rainfall intensity to calculate the average time at which rainfall occurs during the event, normalised between 0 and 1; the *temporal standard deviation*, which measures the spread of rainfall in time around this temporal mean, indicating how temporally concentrated or dispersed the rainfall is over the event duration; the *temporal skewness*, which measures the asymmetry of rainfall in time around this *temporal mean*; and the *temporal kurtosis*, which quantifies how sharply the rain is clustered around that centre.

The full list of metrics applied, including those from the literature alongside additional statistical and temporal moments, is presented in Table 2. The full codebase for rainfall event extraction and metric calculation is openly available at our GitHub repository (https://github.com/masher92/MetricEvaluation/), providing a consistent and reproducible framework for future applications of these metrics.

${\bf 3.5}\quad Testing\ sensitivity\ to\ temporal\ aggregation\ (RQ2)$

To assess the sensitivity of each metric to temporal aggregation of rainfall data, we compare metric values computed on rainfall events derived from data aggregated at different temporal resolutions. We treat metrics computed on events from 5-minute rainfall data as the reference ('truth') and compare them to values obtained from coarser aggregations at 10-, 30-, and 60-minute intervals.





Table 2. List of metrics within each typology applied in this research

Metric type	Metrics			
Classification	3rd / 4th / 5th with peak;			
	3rd/4th/5th with most;			
	3rd with D_{50} ; 3rd with CoG .			
Summary statistics	Max intensity; 130; Cv; (C) skewness; (C) kurtosis; mean intensity; (C) std; (T			
	skewness; (T) kurtosis; (T) std; Centre of gravity; Peak-position ratio; time to			
	peak; Peak-mean ratio; Relative amplitude; Skewp; NRMSEp; Gini coefficient;			
	Lorenz asymmetry coefficient; Event loading index; Fraction of rainfall in Q1 /			
	Q2 / Q3 / Q4; m1; m2; m3; m4; m5; T25; T50; T75; PCI, TCI; Mean intensity			
	HIZ; % time in LIZ / HIZ; % Rain in HIZ.			
Intermittency metrics	Intermittency fraction; Event-dry ratio.			

For each metric and resolution pair, we quantify both numerical and ranking sensitivity. These two complementary measures allow us to distinguish between metrics which exhibit substantial changes in raw values (numerical sensitivity), those which show shifts in the relative ordering of events (ranking sensitivity), and those which display both or neither aspect of sensitivity.

For continuous metrics, the numerical sensitivity is assessed using the symmetrical median absolute percentage error (sMAPE)

(Makridakis and Hibon, 1995). sMAPE measures the absolute percentage error between the metric values at 5 minute and at coarser resolutions, and is calculated as:

$$sMAPE = \frac{100}{n} \sum_{i=1}^{n} \frac{|x_i - y_i|}{(|x_i| + |y_i|)/2}$$
(1)

where x_i and y_i are the original and transformed metric values for event i, respectively.

The ranking sensitivity is assessed using Spearman's rank correlation coefficient (ρ), which quantifies the degree to which the relative ordering of events changes due to temporal aggregation, and is calculated as:

$$\rho = 1 - \frac{6\sum_{i=1}^{n} d_i^2}{n(n^2 - 1)} \tag{2}$$

where n is the number of paired observations, $d_i = R(x_i) - R(y_i)$ is the difference between the ranks of the ith pair of observations.

For categorical metrics, the % of events in a different category from 5 minute at each coarser resolution is used for numerical sensitivity, and Kendall's τ quantifies the ranking sensitivity (Kendall, 1938) by measuring the association between two ranked variables. It is defined as:



345

355

360



$$\tau = \frac{P - Q}{\sqrt{(P + Q + T)(P + Q + U)}}\tag{3}$$

where P / Q are the number of concordant / discordant pairs, and T is the number of ties only in x, and U is the number of ties only in y. If a tie occurs in both x and y for the same pair, it is not counted in either T or U.

We also visually explore how each metric responds to aggregation by plotting distributions across resolutions (using histograms for continuous metrics, and bar plots for categorical metrics).

3.6 Testing sensitivity to normalisation (RQ3)

To evaluate the robustness of rainfall metrics to dimensionless mass curve (DMC) conversion, we compare values calculated on raw 5-minute rainfall events and DMC-transformed rainfall time series. Note that, I30 cannot be calculated, as DMCs have no concept of 30-minutes. Likewise the Frac. in Q1/2/3/4 can only be calculated on events with n timesteps divisible by 4, and so are not calculated either. Following the methods for temporal aggregation sensitivity testing (Sect. 3.5), we calculate numerical and ranking sensitivity of continuous metrics using sMAPE and Spearman's p, and for categorical metrics using % differences in categorisation and Kendall's τ . Metric value distributions are also compared using histograms for continuous metrics, and bar plots for categorical metrics.

350 3.7 Testing metric redundancy and complementarity (RQ4)

To identify metrics which are strongly correlated and which may therefore be considered redundant or interchangeable, we apply agglomerative hierarchical clustering based on pairwise metric similarity across all events (Jain et al., 1999). Similarity between metrics is quantified using the absolute Spearman rank correlation coefficient, and clustering is performed using average linkage. While clustering directly on metric vectors using Euclidean distance was considered, this would have prioritised numerical proximity over functional similarity. This is problematic because some metrics which have very high negative correlation, and likely describe the same feature, are very distant in Euclidean space. Prior to clustering, each metric is assessed for skewness, and those with an absolute skewness <=1 are retained in their original form. For variables with higher skewness, a logarithmic transformation (log1p) is applied if all values are positive, and otherwise, the Yeo-Johnson transformation (Yeo and Johnson, 2000), which supports zero and negative values, is used. After transformation, all variables are MinMax scaled to common [0,1] range. To inform the number of clusters, we compute silhouette scores for a range of candidate cluster numbers. Silhouette scores quantify how appropriate a cluster number is based on how well each metric fits within its assigned cluster, based upon its similarity to members of its own cluster compared with its dissimilarity to those in other neighbouring clusters (Rousseeuw, 1987). This analysis suggests twelve clusters to be the optimal number.



365

370

375

380

385

390

395



4 Results and discussion: Quantitative metric analysis

4.1 Sensitivity to temporal aggregation (RQ2)

The sensitivity of each temporal loading metric to changes in the temporal resolution of the rainfall data is examined in Figure 5. Metrics located in the bottom-right corner of their plot have high robustness (low numerical and ranking sensitivity), whereas those trending upwards and to the left show increasing sensitivity to aggregation. These results are supported by Figure 6, which shows histograms of metric values across all events, with overlain distributions for each temporal resolution. Robustness varies substantially, pointing to meaningful patterns in behaviour.

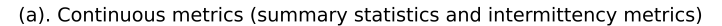
Metrics that describe the peak intensity of rainfall events consistently display a low numerical robustness to temporal aggregation in Figure 5. This includes metrics such as the *peak-mean ratio* and *relative amplitude*, which compare the magnitude of the peak to the overall average intensity. As the temporal resolution becomes coarser, these metrics are distorted because, while the event mean remains relatively stable, the peak intensity is often smoothed, causing the relative peak intensity to decrease. This effect is visible in Figure 6, where distributions for the *relative amplitude*, *peak-mean ratio* and *maximum intensity* shift towards lower values at coarser resolutions. Low numerical robustness is also seen in Figure 5 for m2, the % of rainfall in the whole event found in the peak time-step. However, in this case, the distribution in Figure 6 shifts in the opposite direction, towards higher values. This reflects coarser aggregations having larger time-steps, meaning that the highest-intensity interval captures a larger fraction of rainfall. While these peak intensity-based metrics exhibit high numerical sensitivity to temporal aggregation, their ranking sensitivity remains comparatively low, as evidenced by Spearman's ρ values exceeding 0.8 for all metrics discussed. This indicates that although absolute values change with resolution, the relative ordering of events is largely preserved, suggesting that such metrics may still be useful for comparative analyses, even when temporal resolution varies.

Metrics that describe the timing or position of the peak, such as time to peak and peak-position-ratio, or that are anchored to the timing of the peak, such as m1, event loading index and $skew_p$, are also sensitive to resolution. In contrast to the peak intensity metrics, however, these timing-based metrics show both high numerical and ranking sensitivity. This is expected, as temporal aggregation not only smooths peak intensities but can also displace the perceived timing of the peak. In particular, where the aggregation process assigns aggregated values to the end of time intervals, the peak can be effectively shifted later in time at coarser resolutions. Figure 6 shows broader, more variable distributions for these metrics under coarser resolutions, reflecting increased distortion. A similar pattern holds for categorical metrics. Those that classify events based on the fraction containing the peak rainfall (3rd with peak, 5th with peak) exhibit greater sensitivity to resolution changes than those based on the fraction containing the bulk of rainfall (3rd with most, 4th with most, 5th with most). This suggests that metrics tied closely to the peak are generally more resolution-dependent, while metrics reflecting broader event structure tend to be more robust.

The statistical moments *classical skewness* and *classical kurtosis* both show high numerical and ranking sensitivity to temporal aggregation in Figure 5. As seen in Figure 6, their distributions shift leftward at coarser resolutions, suggesting that rainfall events appear more symmetrical and less heavy-tailed. This reflects the mathematical sensitivity of these moments to extreme values and their positions within the distribution, features that are especially affected by aggregation. Smoothing sharp, intense







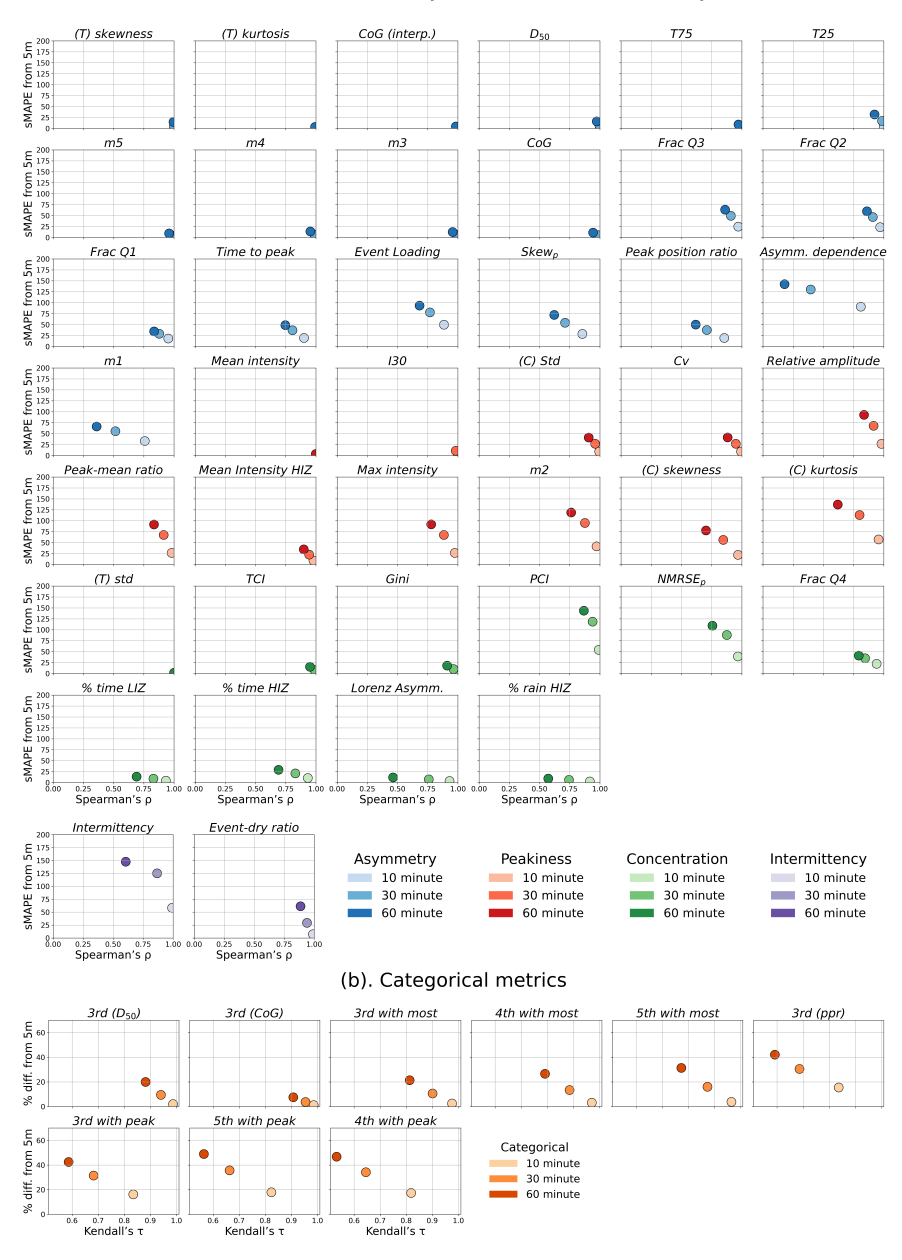


Figure 5. Sensitivity of metrics to temporal aggregation. For each metric (separate subplot), points represent comparisons between the metric calculated at coarser resolutions (10-, 30-, 60-minutes) and the reference 5-minute data. For (a). continuous metrics (summary statistics and intermittency metrics), the x-axis shows Spearman's rank correlation coefficient (p) and y-axis symmetrical mean absolute percentage error (sMAPE) relative to the 5-minute baseline. For (b). categorical metrics, the x-axis shows Kendall's tau, and y-axis shows the percent disagreement with 5-minute baseline.



400

405



peaks reduces the extremity of the tails (lowering kurtosis), while averaging over longer intervals can flatten sharp rises or falls in intensity, reducing asymmetry in the distribution of intensity values (lowering skewness). Ranking sensitivity is also high, as aggregation can reorder events by altering the prominence of subtle asymmetries or outliers.

Metrics that split events into high- and low-intensity zones (HIZ / LIZ) show moderate ranking sensitivity, but fairly low numerical sensitivity (Figure 5). The distribution of % time in HIZ shifts right at coarser resolutions, while for % time in LIZ it shifts left. A higher proportion of time above the mean intensity at coarser resolutions suggests that fewer time steps fall below the mean when extremes are smoothed (and the mean is lower). The % rainfall in HIZ shows less change across resolutions. Its distribution is already heavily skewed toward high values, and aggregation slightly lowers the upper tail, suggesting fewer extreme values, but does not substantially alter the metric's central tendency. The mean intensity in HIZ is relatively robust across resolutions.

The highest robustness in Figure 5 is observed for the time-based moments, including *temporal skewness*, *temporal kurtosis*, *temporal std*, and *centre of gravity*, and percentile timing metrics like D_{50} and T75. These summarise the overall timing and distribution of rainfall across the event, which is less affected by resolution changes than short-lived peaks. Their distributions in Figure 6 remain tightly clustered and largely unchanged across resolutions. Categorical metrics based on these values, such as the 3rd with D_{50} , or the 3rd with CoG, also show the greatest stability among categorical approaches.

Together, Figures 5 and 6 indicate that metrics capturing the cumulative structure and timing of rainfall events can be used with confidence even when only coarse resolution data are available. By contrast, those reliant on the timing or magnitude of short-lived intensity bursts should be applied with caution in such cases.

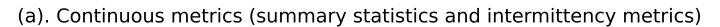
4.2 Sensitivity to normalisation (RQ3)

Sensitivity to conversion of raw 5-minute rainfall into double-normalised, 10-step representations (DMCs) varies substantially across temporal loading metrics, as shown in Figure 7 and Figure 8. As with temporal aggregation (Section 4.1), metrics that describe the overall distribution of rainfall over time show the least sensitivity to normalisation. In Figure 7a, these robust metrics cluster in the bottom-right and are shown in more detail in the inset. They include mass distribution indicators (m3, m4, m5), percentile timing metrics (T25, D/T50, T75), and moment-based metrics ($centre\ of\ gravity$, $temporal\ skewness$, and $temporal\ kurtosis$). The value distributions for these metrics in Figure 8 also remain largely unchanged after DMC conversion. These metrics are inherently robust to both interpolation and loss of dimensionality because they reflect the shape and balance of the event over its duration, rather than relying on specific peaks or absolute magnitudes. Their values are either unitless by construction or meaningful when expressed as proportions of total event time or mass, making them more stable across transformations. Categorical metrics based on these values, such as the $3rd\ with\ D_{50}$, or $3rd\ with\ CoG$, as well as those recording the fraction with most rainfall ($3rd\ /\ 4th\ /\ 5th\ with\ most$), also show the greatest stability among categorical approaches (Figure 7, Figure 8).

By contrast, several metrics that take continuous values on raw rainfall series become discretised when applied to DMCs interpolated to only 10 time steps. These include % time in LIZ / HIZ, event dry ratio, intermittency, peak-position-ratio, centre of gravity, skew_p, and classical skewness. These depend on the proportion of event time spent above or below certain







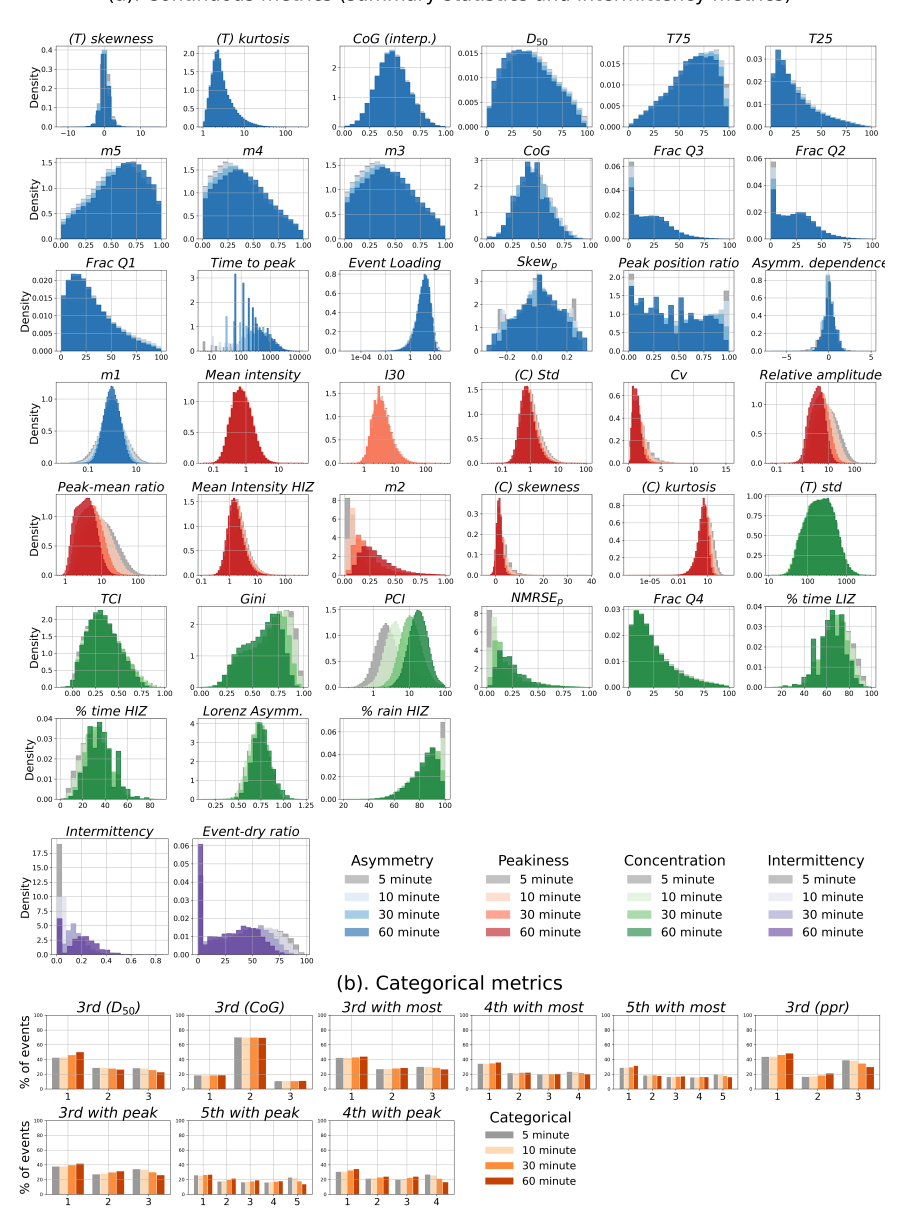


Figure 6. Sensitivity of metric distributions to temporal aggregation. Each subplot shows how the distribution of a given metric changes when calculated on rainfall data at different temporal resolutions (5-, 10-, 30-, 60-minutes). For (a). continuous metrics, this is shown using overlaid histograms. For (b). categorical metrics, grouped bar charts display the relative frequency of each category across resolutions.



435

440



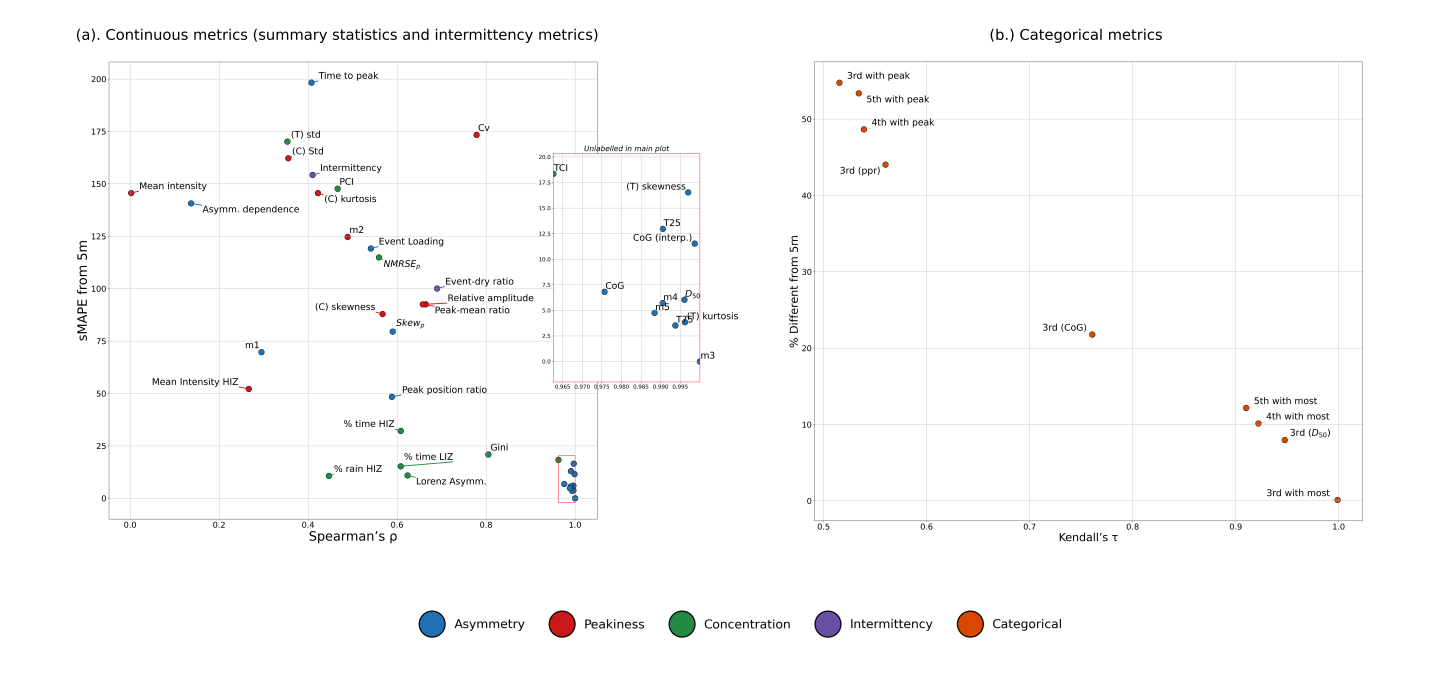


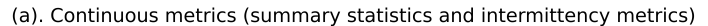
Figure 7. Sensitivity of metrics to dimensionless mass curve representation. For each metric, points represent comparisons between the metric calculated with 5-minute raw data and with a 10-point, DMCs calculated on 5-minute data. For (a). continuous metrics (including summary statistics and intermittency metrics), the x-axis shows Spearman's rank correlation coefficient (*p*) and y-axis the symmetrical mean absolute percentage error (sMAPE). For (b). categorical metrics, the x-axis shows Kendall's tau and the y-axis the percent disagreement between the pairs of metric values.

thresholds or in specific zones, and so are limited in the DMC to multiples of 10%, constraining meaningful variation in range and granularity across events. This is very apparent in the stepped histograms of these metrics in Figure 8a Similarly, the interpolation used in the DMC conversion introduces a form of resolution coarsening similar to temporal aggregation. As with coarser time steps, this process smooths sharp transitions and reduces variability, disproportionately affecting metrics that are sensitive to peak timing and magnitude, such as *peak-mean ratio*, *relative amplitude*, *peak-position-ratio*, *m1*, *m2*, and the *event loading index*.

However, the effects of DMC transformation extend beyond temporal smoothing. Unlike temporal aggregation, DMC conversion involves full de-dimensionalisation, with both time and intensity rescaled to a [0,1] domain. This has more severe consequences for metrics that rely on real physical quantities. For instance, *mean intensity* becomes meaningless, as the total intensity is fixed to 1, and so the mean intensity is 0.1 in all cases (Figure 8a). Similarly, metrics that rely on absolute intensity contrasts, such as the *standard deviation* or *coefficient of variation*, lose interpretability when all intensities are normalised. In these cases, relative differences are compressed and the metric no longer reflects the original signal.







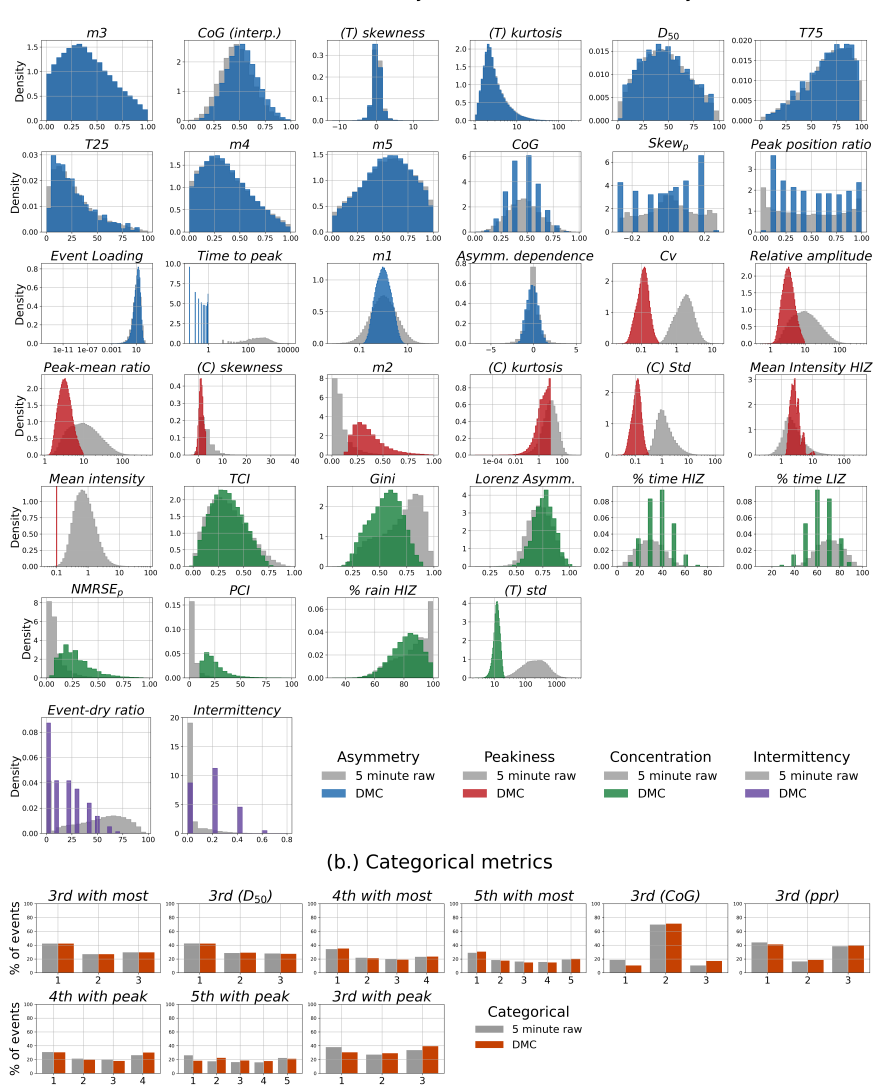


Figure 8. Sensitivity of metric distributions to double normalisation in DMCs. Each subplot shows how the distribution of a given metric changes when calculated on raw rainfall data at 5-minute temporal resolution and on a double-normalised version of the event, interpolated to ten data points. For (a). continuous metrics, distributions are shown using overlaid histograms. Note that gaps in some histograms arise from the discretisation of values when metrics are computed on DMCs—certain metric values are simply not possible, so some histogram bins remain empty. For (b). categorical metrics, grouped bar charts show the relative frequency of each category across resolutions.



455

460

465



This distinction is particularly important when DMCs are used to generate synthetic events or inform design storms. In these cases, dimensionless curves are often re-scaled using external information about storm depth and duration to reconstruct plausible, physically realistic events. Metrics that remain interpretable in the dimensionless domain are therefore better suited to characterising DMC shapes or classifying rainfall types, while those that depend on physical units or fine-grained temporal variation may require adaptation or caution when applied to normalised forms.

Taken together, these findings underscore the importance of considering input representation when comparing rainfall met450 rics across studies, particularly when simplifications like DMCs are involved. Metrics that are robust to DMC transformation
may be more appropriate for comparative analysis or pattern identification, while others may require adjusted interpretation
when removed from their physical context.

4.3 Metric redundancy and complementarity (RQ4)

Figure 9a plots a dendrogram which visualises the results of hierarchical cluster analysis based on the similarity between each pair of temporal loading metrics across the rainfall event dataset. The horizontal distance between each metric and where it joins with another branch represents similarity, with items merging at shorter distances being more similar. Twelve clusters are used, which was indicated in silhouette score analysis to be the optimal number to increase in-group cohesion, and reduce between-group separation (see Figure D1, Appendix D). On the dendrogram, the clusters containing more than one metric are coloured and labelled with a cluster number. The resulting clusters reveal groups of metrics that behave similarly across events and may therefore capture overlapping or redundant structural information.

Cluster 1 is the largest cluster, with fifteen metrics, and relates to the timing of mass distribution. This includes classification metrics (3rd with most, 4th with most, 5th with most, 3rd with D_{50} and 3rd with CoG), as well as percentile-based metrics (T25, T50, T75), mass-distribution indicators (m4, m3, m5), temporal skewness, the centre of gravity, and the fraction of rainfall in Q1. This cluster contains metrics with the strongest (positive or negative) correlations, as can be seen in Figure 9b which plots the Spearman's correlation matrix. Negative correlations arise where metrics respond to the same underlying asymmetry but with reversed directionality. For instance, a front-loaded event will have a lower D_{50} , but a higher m3 (proportion of rainfall in the first third). The high correlations between metrics in the cluster suggests that these metrics can be used interchangeably to rank the asymmetry in rainfall mass distribution in a set of rainfall events.

Cluster 2 contains a grouping of eight metrics clearly related to the timing of the peak timestep. Metrics in this peak timing cluster include several classification metrics (e.g. 3rd with peak, 4th with peak, 5th with peak, and 3rd (D₅₀)), as well as summary statistics that explicitly quantify peak position (e.g., peak-position-ratio, time-to-peak, and skew_p). Interestingly, the metric m1, representing the ratio of rainfall before versus after the peak, is also placed within this cluster. Although m1 is seemingly focused on the balance of rainfall mass distribution rather than peak timing, its position within this cluster suggests that, in practice, it is strongly influenced by peak placement. Cluster 2 appearing adjacent to, but distinct from, cluster 1 implies that while both peak and mass timing relate to the temporal distribution of rainfall, they are not completely interchangeable concepts. This highlights the importance of establishing the aspect of temporal loading most relevant to a specific application before selecting metrics to utilise.



480

485



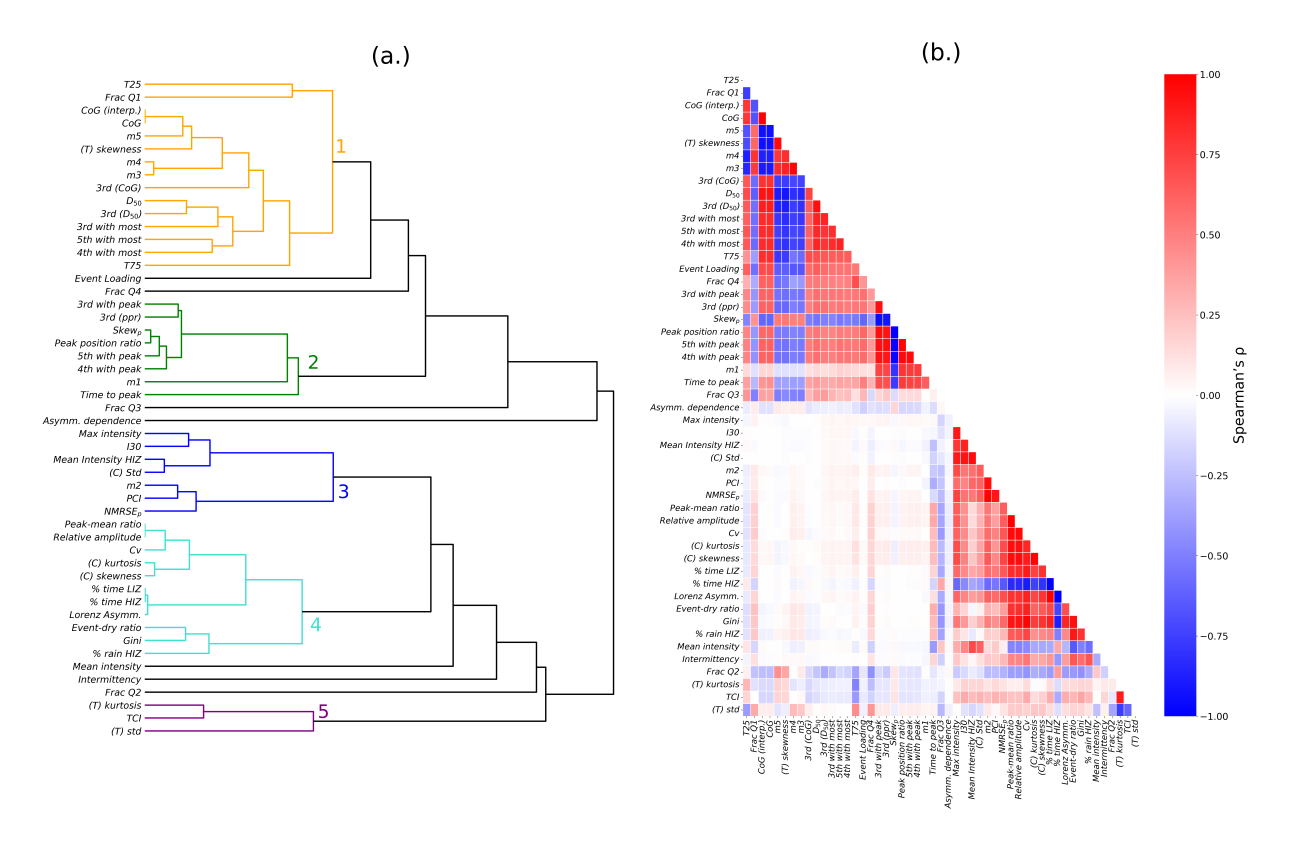


Figure 9. (a) Dendrogram visualising results of hierarchical cluster analysis of the pairwise similarity of metrics across all events. Similarity is quantified using the absolute value of Spearman's ρ , and clustering is performed using agglomerative hierarchical clustering with average linkage and 12 clusters. Clusters with more than one member are highlighted in red and marked with a cluster number. (b) The full Spearman correlation matrix upon which clustering is based

Unlike the first two clusters, which both capture aspects of when rainfall occurs within the event, whether in terms of the distribution of mass or the relative timing of the peak, the metrics in the third, fourth and fifth clusters are not concerned with sequencing in time. Instead, they describe the magnitude of the peaks and how rainfall is concentrated among timesteps (magnitude concentration), and for some metrics, how closely such high-intensity timesteps occur (temporal concentration), without distinguishing whether these bursts fall early, mid, or late in the event.

The third and fourth clusters contain metrics relating to the peak magnitude and magnitude concentration. In cluster 3, the first of the three subclusters identified on the dendrogram is formed by *maximum intensity* and *I30* (the maximum intensity in any 30-minute period). These both capture the magnitude of the single wettest short-duration period without reference to the rest of the event. The second subcluster groups the *mean intensity in the HIZ* (timesteps above the event's mean intensity) with *classical standard deviation* (the variation of rainfall intensities around the mean intensity). Both metrics emphasise how rainfall is distributed relative to the event mean, reflecting the degree to which rainfall is concentrated into particularly intense phases as opposed to being spread more evenly across the event. The third subcluster contains *m2* (percentage of total rainfall



500

505

520



in the highest-intensity timestep), *PCI*, and *NRMSE_p*. These metrics explicitly compare rainfall in some timesteps with rainfall in others, directly quantifying how concentrated rainfall is within an event. They also share a potential sensitivity to event length, tending to return higher values when an intense burst is embedded in a short event than when it appears in a longer event with more low-intensity timesteps. Taken together, the three subclusters demonstrate that cluster 3 relates to metrics of storm magnitude and concentration. The first subcluster isolates the absolute peak intensity, while the second and third reflect different ways of capturing how rainfall is concentrated across timesteps. Events with very high peaks often also display strong contrasts between high- and low-intensity periods, which is consistent with the behaviour of concentration-focused metrics such as *mean intensity in the HIZ*, (*C*) *std*, *m2*, *PCI*, and *NRMSE_p*.

Cluster 4 relates to magnitude concentration, but focuses more on metrics that reflect distributional imbalance, showing how rainfall is unevenly shared across timesteps rather than simply reflecting the size of absolute peaks. The first subcluster captures how rainfall peaks dominate relative to the event average. *Peak—mean ratio* and *relative amplitude* form a tight group, both measuring peak intensity relative to the mean, while their association with the *coefficient of variation (CV)* reflects the shared emphasis on mean-based ratios. Although *CV* compares the mean to the standard deviation rather than the peak directly, the standard deviation rises sharply as peaks intensify, highlighting the contrast between intense and weaker timesteps. The second subcluster contains the moment-based descriptors *(C) kurtosis* and *(C) skewness*, which characterise the shape of the rainfall distribution. As negative kurtosis is rare in rainfall events (as this would involve lots of high intensity timesteps, accompanied by few low intensity), skewness and kurtosis generally co-vary. Both metrics tend to be high in events with rainfall concentrated in a few time steps, and low in more uniform events. Another subcluster tightly links the *% time in LIZ* with its complement, *% time in HIZ*, reflecting their inverse relationship, with *Lorenz asymmetry* joining nearby as it also quantifies imbalance in the rainfall distribution between wetter and drier periods. In a separate branch, *event-dry ratio*, *Gini coefficient*, and *% of rainfall in the HIZ* cluster together, collectively describing how rainfall volume concentrates into a few timesteps, with events scoring high on one metric tending to do so on the others as well.

The fifth cluster in Figure 9.a groups *temporal kurtosis*, *temporal standard deviation*, and the *TCI*, all of which quantify the temporal concentration of rainfall. Unlike magnitude-based concentration metrics, these measures only return high values when high-intensity timesteps are tightly grouped in time. Their very low correlation with other metrics indicates that this dimension of temporal loading is largely independent from others. This property is particularly relevant for applications such as flash-flood risk assessment and soil erosion modelling, where closely clustered high-intensity periods can greatly amplify impacts compared to if high intensity timesteps were spread across an event.

The remaining seven 'clusters' each contain only a single metric. In some cases this suggests they provide unique information about rainfall events. The *asymmetry of dependence* characterises how rainfall intensities evolve over time, identifying whether events increase and decrease in intensity at similar rates, a feature that may be relevant for understanding event evolution or storm generation. In Figure 9a, this metric is shown to split off very early from the other metrics, highlighting its unique position. The *event loading index* measures the deviation in temporal variability between an observed rainfall event and a version of that event but mirrored in time. This captures structural irregularities not represented by other metrics, although its conceptual similarity to asymmetry is reflected in its positioning between the asymmetry focused 1st and 2nd clusters.





Likewise, *intermittency* captures the frequency with which rainfall starts and stops during an event, a feature not reported by other metrics. In contrast, the isolated clustering of the fractional metrics, *fraction rainfall in Q2*, *Q3*, and *Q4*, more likely reflects their limited descriptive power when considered individually. Unless one quarter dominates the rainfall distribution, these metrics tend not to strongly distinguish between different event types or structures. Similarly, *mean intensity* does not intuitively convey any information about temporal loading. It is included in this analysis to test whether any other metrics are implicitly driven by the total event scale. This appears to not be the case, which is a useful conclusion. These results highlight the importance of selecting a diverse set of metrics when analysing rainfall temporal loading. While many metrics are highly interrelated, a subset offer complementary insights that may enhance interpretation or predictive performance when used together.

5 Recommendations

A central contribution of this paper is the argument that analyses of rainfall temporal loading must begin with a clear definition of the aspect(s) most relevant to the research question or application. Rather than prescribing a single universal metric, we provide a conceptual framework to guide deliberate, defensible, and replicable metric selection. Based on the findings of the literature review and the data-driven clustering exercise, we recommend breaking event temporal loading into five components: (1) mass timing, (2) peak timing, (3) magnitude concentration, (4) temporal concentration, and (5) intermittency. In Table 3, for each component we summarise its meaning, list all associated metrics and indicate one suggested metric.

Our analysis shows that many metrics are sensitive to temporal resolution or DMC transformations. For peak timing, magnitude concentration, and intermittency, no metrics are fully robust, reflecting the inherent variability of peaks and the smoothing introduced by temporal aggregation. We highlight that this means that studies using these metrics across different resolutions should interpret comparisons with caution. For these components, we recommend use of metrics which have been more commonly applied in the past and which are conceptually simple. Temporal concentration and mass timing metrics are generally more robust. For these components, our recommended metrics also consider simplicity and prior usage in the literature, in addition to robustness. While we highlight the 'robust' metrics in Table 3, we note that Tables C1, C2 and C3 in Appendix C. provides full metric-specific summaries of robustness.

6 Summary and conclusions

545

This study provides a comprehensive review and empirical analysis of rainfall event temporal loading metrics, drawing on literature from multiple domains including flood modelling, soil erosion and sediment transport, pollution modelling, landslide prediction, and climate change impact assessment. We identify 52 metrics that have been used to describe the temporal distribution of rainfall within storms, and apply these to over 233,000 events observed by a large network of rain gauges. This represents the first large-scale, systematic evaluation of how such metrics behave across real-world rainfall events.





Table 3. Five recommended components of rainfall event temporal loading. Each component is accompanied by its definition and a list of all reviewed metrics which are best described by this component, with metrics found to be robust at different temporal resolutions and after DMC normalisation highlighted in red. A recommended metric for use studying each component is also provided.

Category	Description	All metrics	Recommendation	on Reasons
Mass timing	Describes when the majority of rainfall mass falls during the event. From the start (low values), through the middle, to the end (high values).	3rd / 4th / 5th with most, 3rd with D ₅₀ , 3rd with CoG, Centre of gravity, D ₅₀ , T25/75, m1, m3, m4, m5, Event loading index, (T) skewness, Asymmetry of dependence, Frac. in Q1 / 2 / 3 / 4	4th with most (categorical) D ₅₀ (continuous)	Of the robust metrics, these ones have been most commonly applied previously
Peak timing	Describes when the peak intensity occurs during the event. From the start (low values), through the middle, to the end (high values).	3rd/4th/5th with peak, 3rd ppr, time-to-peak, peak-position-ratio, Skew _p	Peak-position- ratio	No peak timing metrics are robust, so use in cross-study comparison with care. <i>Peak-position-ratio</i> is the most widely applied, easily understood option.
Magnitude concentra- tion	Describes the strength of intense phases, contrasts between high- and low-intensity periods, or overall statistical inequality. Not affected by whether timesteps concentrating rainfall are close together in time, or where in time they occur.	Max intensity, I30, PCI, (C) skewness, (C) kurtosis, (C) std, CV, Mean intensity in HIZ, % time in LIZ/ HIZ, % Rain in HIZ, Gini Coefficient, Lorenz Asymmetry Coefficient, NRMSE _p , Peak-mean ratio, Relative amplitude, m2	Gini coefficient	Gini coefficient is the only metric robust to both temporal resolution and DMC transformation.
Temporal concentra- tion	Describes how narrowly rainfall is clustered around a point in time, regardless of when in time that cluster appears.	TCI, T (kurtosis), T (std)	(T) std	All metrics are robust. While <i>TCI</i> has been used previously in one study, we recommend that <i>T</i> (<i>std</i>) is a simpler metric to measure the same property.
Intermittency	Describes how intermittent rainfall is within the event.	Intermittency fraction, Event dry ratio	Event dry ratio	Neither are robust across resolutions and so should be used in cross-study comparison with care. Both metrics have only been applied once previously, but the <i>event-dry ratio</i> is conceptually simpler.



555

560

565

570

575

580

585



We begin by organising the metrics with a typology that groups metrics into three broad categories: (i) classification metrics, which assign events to discrete categories; (ii) summary statistics, which generate continuous descriptors of temporal loading; and (iii) intermittency metrics, which quantify the frequency and spacing of dry intervals within an event. This typology is constructed based primarily on metric form (e.g. categorical versus continuous) and purpose. We then perform a data-driven hierarchical cluster analysis that reveals further groups of metrics that transcend these categories. Notably, two well-defined groups of metrics are identified, including one capturing the timing of peak intensity and another describing the timing of rainfall mass distribution. Each includes both summary statistics and classification metrics, suggesting that despite differences in format, these metrics capture similar underlying aspects of temporal loading and tend to rank events similarly, indicating a degree of interchangeability for comparative purposes. However, we note that this does not necessarily imply that metric choice within these clusters will not materially alter overall findings. For instance, an analysis based on the 3rd with most rainfall may conclude differently on whether a geographical area generally has a tendency towards front-loaded events, than if D_{50} is the chosen metric. Exploring how variations in absolute metric values within correlated groups may alter substantive conclusions was beyond the scope of this study, but we highlight it as a valuable focus for future research.

The cluster analysis also reveals several looser groupings and a number of isolated metrics. This reflects a broader issue that many metrics used under the banner of 'temporal loading' in fact represent quite different concepts. This can lead to metrics being borrowed across domains without clear understanding of whether the metric is actually appropriate for the intended application. To address this, we propose a conceptual framework that distils our findings into five aspects of temporal loading: (1) mass timing, (2) peak timing, (3) magnitude concentration, (4) temporal concentration, and (5) intermittency. The choice of these five aspects is motivated by a combination of statistical evidence, existing practice, and conceptual need. Clarifying and standardising these concepts represents a critical step toward improving comparability and interpretability across studies.

We note that comparing metrics across different data types, particularly continuous summary statistics and discrete categories, introduces interpretive limitations. When calculating sMAPE scores and plotting metric distributions we opted to not transform or scale metrics. This was to preserve the physical interpretability of each metric, allowing percentage errors to reflect changes in real units (e.g., minutes or intensity proportions) rather than abstracted or standardised values. However, although sMAPE expresses the average percentage difference between two representations (e.g., at different resolutions), the meaning of a given percentage depends on the nature and scale of the metric. For instance, a 70% sMAPE for a bounded percentile-based timing measure like D₅₀ does not carry the same meaning as a 70% sMAPE for a scale-dependent metric such as standard deviation. This presents a trade-off, where preserving metric-specific meaning improves interpretability within each metric, but complicates comparative analysis across them. We recognise that we are operating within these constraints, but by interpreting sMAPE scores in conjunction with visual plots, rank correlations, and physical understanding of the metric's behaviour, we still make valuable assessments of metric behaviour at different resolutions and processing options.

Our empirical analysis of whether metrics report consistent results when applied to rainfall events at different temporal resolutions and when converted to normalised, dimensionless representations goes some way towards addressing the broader lack of methodological transparency in event temporal loading research. We show that some metrics, especially those based on the peak timing or magnitude, are highly sensitive to temporal resolution, whereas metrics capturing the overall precipitation



605



distribution tend to be more robust. Similar patterns apply for double normalised events, where the reduced number of time steps constrains accurate representation of peaks. Additionally, the de-dimensionalisation process leads to discretisation of some metric values and renders those based on absolute values uninterpretable. While these findings provide practical guidance for selecting appropriate metrics in contexts with limited or pre-processed data, a number of methodological uncertainties remain. In particular, it is often unclear whether metrics should be applied to the full rainfall event or to only the most intense burst.
 Additionally, the treatment of events with multiple peaks, or with no clear peak, remains insufficiently explored. Many metrics assume events have a single dominant peak, but the implications of including or excluding multi-peaked or uniform events in analyses are not well understood. Some research, e.g., Nguyen and Chen (2022), attempts to separate uniform rainfall events, using the Schutz Index, and to treat these differently. We recommend future research investigate this further, and consider filtering approaches based on peak structure, including the potential exclusion of events with multiple or indistinct peaks, to
 ensure appropriate and meaningful application of temporal loading metrics.

Finally, it is important to reflect on the representativeness of the rainfall data used in this study. Our analysis draws on the high-quality, dense network of gauges across Denmark, providing over 233,000 well-observed rainfall events. This scale of dataset allows for robust evaluation of metric behaviour under real storm conditions. However, Denmark's temperate maritime climate is not fully representative of the range of rainfall regimes globally. In particular, strongly convective extremes typical of tropical and subtropical climates are less frequent, and storm dynamics may differ from those in arid or mountainous regions. As such, while our findings on the behaviour, sensitivity, and clustering of metrics are expected to generalise across contexts, the specific distribution of rainfall events and the relative prevalence of different temporal loading structures may not. We therefore recommend that future work apply similar analyses in a wider set of climatic settings, both to test the robustness of our methodological conclusions and to build a more globally representative basis for metric selection.

10 Code availability. Code is available at https://github.com/masher92/MetricEvaluation/

Appendix A: Boolean search query

Scopus supports proximity operators (e.g., W/n requires two words to appear within n words of each other; Pre/n requires one word to precede the other within n words), a feature not available in the other databases. As such, for Scopus the search term was: [(("rainfall event" OR "precipitation event" OR "rain storm" OR "rainstorm" OR "storm event" OR (('precipitation" OR "rain" OR "rainfall" OR "storm") PRE/3 "event")) OR (("precipitation varia*" OR "rainfall varia*") W/1 "intra-event")) W/5 ("rainfall profile" OR "temporal pattern" OR "temporal distribution" OR "event loading" OR "temporal profile" OR "temporal loading" OR "intensity profile" OR (("precipitation pattern" OR "rainfall pattern") W/3 "temporal"))] and for Web of Science and Google Scholar, it was: ("rainfall event" OR "precipitation event" OR "rain storm" OR "rainstorm" OR "storm event" OR ("precipitation" OR "rainfall" OR "rainfall" OR "storm") AND "event" OR ("precipitation varia*" OR "rainfall varia*") AND





"intra-event") AND ("rainfall profile" OR "temporal pattern" OR "temporal distribution" OR "event loading" OR "temporal profile" OR "temporal loading" OR "intensity profile" OR ("precipitation pattern" OR "rainfall pattern") AND "temporal")].





Appendix B: Selected papers

Table B1. Summary of reviewed papers

Authors	Metric type	Metric	Study purpose	Rainfall	Processing
Amin et al. (2000)	Classification	4th with most	Characterising typical profiles in an area	Real	DMC
Aquino et al. (2013)	Classification	3rd with peak	Impact of storm temporal pattern on Real soil erosion		Raw
Asher et al. (2025)	Classification	5th with most	Impact of storm temporal pattern on flood risk	Synthetic	DMC
Azli and Rao (2010)	Classification	4th with most	Characterising typical profiles in an area	Real	DMC
Back and Rodrigues (2021)	Classification	4th with peak	Characterising typical profiles in an area	Real	Unclear
Bezak et al. (2018)	Classification	4th with most	Impact of storm temporal pattern on hydraulic model outcomes	Synthetic	DMC
Brommer et al. (2013)	Summary stats	mean, (C) std, (C) skewness, (C) kurtosis	Characterising typical profiles in an area	Real	Raw
Cai et al. (2024)	Summary stats	Peak-position- ratio, PCI	Impact of storm temporal pattern on peak runoff generation	Synthetic	Raw
Chen et al. (2015)	Classification	4th with most	Characterising typical profiles in an area	Real	Unclear
de Assunção Montenegro et al. (2018)	Classification	3rd with peak	Impact of storm temporal pattern on soil moisture patterns	Real	Raw
de Andrade et al. (2020)	Classification, Summary stats	130, 3rd with peak	<u> </u>		Raw
Dolšak et al. (2016)	Classification	4th with most, BSC	C Characterising typical profiles in an Real area		DMC
Dunkerley (2021b)	Intermittency	Intermittency frac-	Developing methods for describing temporal profile	Real	Raw
Fan et al. (2020)	Summary stats	(C) skewness, (C) kurtosis	Impact of storm temporal pattern on landslides	Synthetic	Raw





Authors	Metric type	Metric	Study purpose	Rainfall	Processing
Fatone et al. (2021)	Classification	3rd with peak	Impact of storm temporal pattern on hydrograph outflow	Real	DMC
Fu et al. (2021)	Summary stats	Coefficient peak rainfall intensity, 3rd with ppr	Impact of typhoon temporal pattern on pollution generation	Real	Raw
Gao et al. (2024)	Summary stats	Relative amplitude	Impact of storm temporal pattern on soil erosion	Real	Raw
García-Bartual and Andrés- Doménech (2017)	Summary stats	(C) kurtosis, (C) standard deviation	Characterising typical profiles in an area	Real	Raw
Garcia-Guzman and Aranda- Oliver (1993)	Classification	4th with most	Characterising typical profiles in an area	Real	DMC
Ghanghas et al. (2024)	Summary stats	Event Loading Index	Impact of climate on temporal pattern	Real	Raw
He et al. (2022)	Summary stats	PCI	Characterising typical profiles in an area	Synthetic	Raw
He et al. (2024)	Summary stats	(C) skewness, (C) kurtosis	Impact of storm temporal pattern on slope instability	Synthetic	Raw
Horner and Jens (1942)	Classification	Third with peak	Impact of storm temporal pattern on surface runoff	Real	Unclear
Hu et al. (2018)	Summary stats	Gini coefficient, Lorenz coefficient	Changes to temporal inequality of daily precipitation over last 50 years	Synthetic	Raw
Huff (1967)	Classification	4th with most	Characterising typical profiles in an area	Real	DMC
Jeon et al. (2017)	Classification	4th with most	Impact of storm temporal pattern on water quality from storm runoff	Synthetic	DMC
Jun et al. (2021)	Summary stats Classification	4th with most, time to peak	Characterising typical profiles in an area	Real	Unclear
Knighton and Walter (2016)	Summary stats	T25 50 75, time to peak	Stochastic event generation	Real	DMC
Li et al. (2023)	Summary stats	Peak-mean ratio, peak-position-ratio	Evaluating satellite precipitation products	Real	Raw
Liang et al. (2023)	Classification	3rd with most	Impact of storm temporal pattern on soil erosion	Synthetic	DMC





Li et al. (2021)	Classification	4th with most	Characterising typical profiles in an	Real	Raw
L1 Ct al. (2021)	Ciassification	+ın wun most	area;	Keai	Naw
			Impact of storm temporal pattern on		
			sewer overflows		
Live et al. (2022)	Cummany atata	Dalatina amalituda		Dool	Daw
Liu et al. (2022)	Summary stats	Relative amplitude,	Impact of storm temporal pattern on	Real	Raw
		% rain HIZ, % time	runoff and soil loss		
		in HIZ / LIZ			
Long et al. (2021)	Summary stats	TCI	Impact of climate on temporal (and	Real	Unclear
			spatial) pattern		
Loveridge et al. (2015)	Classification	3rd with D50	Characterising typical profiles in an	Real	DMC
			area		
Lu and Qin (2020)	Classification	4th with most	Impact of storm temporal pattern on	Synthetic	DMC
			urban drainage		
Müller et al. (2017)	Summary stats	Asymmetry of de-	Impact of storm temporal patterns	Real	Raw
		pendence	on sewer flow simulations		
Nel (2007)	Classification	4th with peak	Characterising typical profiles in an	Real	DMC
			area;		
			Impact of storm temporal pattern on		
			runoff and soil erosion		
Oh et al. (2024)	Summary stats	$NRMSE_p$ and $Skew_p$	Impact of storm temporal pattern on	Real	Unclear
,	•	r	peak flood discharge		
Pinheiro et al. (2018)	Classification	3rd with peak	Characterising typical profiles in an	Real	DMC
, ,			area;		
			Impact of storm temporal pattern on		
			soil erosion		
Pohle et al. (2018)	Summary stats;	Event dry ratio,	Stochastic event generation	Synthetic	Raw
()	Intermittency	Frac. in Q1 / Q2 /			
		Q3 / Q4			
Terranova and Iaquinta (2011)	Classification	BSC	Characterising typical profiles in an	Real	DMC
1011ano (a ana 1aquina (2011)	Siassiffoution	250	area	11041	Direc
Tian et al. (2017)	Summary stats	CV	Stochastic event generation	Synthetic	Raw
Todisco (2014)	Classification	CV, Run number	Developing methods for describing	Real	Raw
1041300 (2017)	Ciassification	Cr, Run number	temporal profile;	icai	ixaw
			Impact of storm temporal pattern on		
m 1 (2005)	al in		soil erosion		D
Tsubo et al. (2005)	Classification	4th with peak	Characterising typical profiles in an	Real	DMC
			area		





Serna and Taipe (2019)	Classification	3rd with peak	Characterising typical profiles in an area	Real	DMC
Schiff (1943)	Classification	3rd with peak	Impact of storm temporal pattern on infiltration and runoff	Real	DMC
Varga et al. (2009)	Classification	3rd with CoG	Developing methods for describing temporal profile	Real	DMC
Vantas et al. (2019)	Classification	4th with most	Developing methods for describing temporal profile	Real	Raw
Villalobos Herrera et al. (2023)	Classification	5th with most	Characterising typical profiles in an area	Real	DMC
Visser et al. (2023)	Summary stats	D_{50}	Impact of climate on temporal pattern	Real	DMC
Wang et al. (2016)	Classification	3rd with peak	Impact of storm temporal pattern on soil erosive loss	Real	DMC
Wang et al. (2018)	Classification	3rd with ppr	Impact of storm temporal pattern on soil water transport	Real	DMC
Yang et al. (2015)	Summary stats	Coefficient of vari- ability	Assessing performance of data assimilation on events with different temporal loading characteristics	Real	Raw
Yang et al. (2022)	Summary stats	Peak-position-ratio	Characterising typical profiles in an area Regional patterns in temporal profile	Real	Raw
Yang et al. (2024)	Classification	5th with peak	Impact of storm temporal pattern on flash flooding	Real	Unclear
Yin et al. (2016)	Classification	4th with peak	Characterising typical profiles in an area	Real	DMC
Wartalska et al. (2020)	Summary stats	m1, m2, m3, m4, m5, peak-position- ratio	Characterising typical profiles in an area	Real	DMC
Wartalska and Kotowski (2020)	Summary stats	$m4, n_i$	Characterising typical profiles in an area; Impact of future climate on typical profiles.	Real	DMC
Williams-Sether (2004)	Classification	4th with most	Characterising typical profiles in an area	Real	DMC





Appendix C: Selected metrics

Table C1. Summary of reviewed metrics (Part 1: Classification)

Metric	Meaning	Focus		Robust to:
			Temp res DMC transforma	
3rd/4th/5th with peak	Fraction of event with peak rainfall	Peak timing	×	×
3rd/4th/5th with most	Fraction of event with most rainfall	Asymmetry	\checkmark	✓
$3rd$ with D_{50}	Third in which 50% of rainfall is reached	Asymmetry	\checkmark	✓
3rd with CoG	Third containing centre of gravity of rainfall	Asymmetry	✓	✓





Table C2. Summary of reviewed metrics (Part 2: Summary statistics)

Metric	Meaning	Focus		Robust to:
			Temp res	DMC transformation
	Peakiness indicators			
Max intensity	Maximum rainfall intensity	Peakiness	×	×
Mean intensity	Mean rainfall intensity	Peakiness	✓	×
<i>I30</i>	Max rainfall depth in any 30-minute period	Peakiness	✓	×
Classical (C) std	Standard deviation: variation of rainfall intensity	Peakiness	✓	×
	values around mean intensity			
Cv	Coefficient of variation (std/mean): standardised	Peakiness	✓	×
	variation of intensity values around mean intensity			
Classical (C) skewness	Asymmetry of intensity value distribution. + skew-	Peakiness	×	×
	ness indicates most values small, some big, - skew-			
	ness indicates most values big, some small.			
Classical (C) kurtosis	Tailedness of intensity value distribution. + kur-	Peakiness	×	×
	tosis indicates sharp, intense bursts concentrated			
	in short periods, - kurtosis reflects rainfall spread			
	more evenly over time without extreme peaks.			
Peak-mean ratio / Rainfall	Peak-to-mean ratio: maximum intensity divided by	Peakiness	×	×
intensity irregularity (n_i)	mean intensity			
Relative amplitude (R _{am})	Range divided by mean	Peakiness	×	×
m2	% rainfall in highest-intensity time step / rainfall in	Peakiness	×	×
	whole event			
Mean intensity in HIZ	Average intensity during above-average intensity	Peakiness	✓	×
	periods			
	Asymmetry indicator	rs		
Time to peak	Time to peak in minutes	Peak timing	×	×
Peak-position-ratio /	Time to peak divided by duration	Peak timing	×	×
coefficient-peak-rainfall-				
intensity)				
$Skew_p$	Value from -0.25 to 0.25 measuring relative position	Peak timing	×	×
	of peak within rainfall duration indicates front-			
	loading, + indicates back-loading.			
T25 / T50 and D ₅₀ / T75	Percent of event passed when X% of rainfall hap-	Asymmetry of	✓	✓
	pened	rainfall		
m3 / m4 / m5	% rainfall in first 33% / 30% / 50% of event duration	Asymmetry of	✓	✓
		rainfall		





Metric	Meaning	Focus	Robust to:		
			Temp res	DMC transformation	
m1	Relative volume of rainfall before versus after the	Asymmetry of	×	×	
	peak	rainfall			
Centre of gravity (CoG)	Timing of rainfall mass centre, snapped to nearest	Asymmetry of	✓	√	
	time step	rainfall			
Centre of gravity (interpo-	Fractional timing of rainfall mass centre across	Asymmetry of	✓	✓	
lated) (CoG interp.)	event duration	rainfall			
Event loading index	Comparison of temporal variability (captured by	Asymmetry of	×	×	
	the standardised temporal heterogeneity, STH) of a	rainfall			
	storm against that of a symmetrised version con-				
	structed by mirroring the rising limb around the				
	peak.				
Asymmetry of dependence	Describes the degree of reversibility in a timeseries	Asymmetry of	×	×	
	using ranked-based statistics (copulas)	rainfall			
Temporal (T) skewness	Skewness of rainfall distribution considered over	Asymmetry of	\checkmark	\checkmark	
	$time-more\ front-loaded, +more\ back-loaded$	rainfall			
	Concentration indicate	ors			
Precipitation Concentra-	Compares sum of squared intensities to square of	Magnitude con-	×	×	
tion Index (PCI)	total rainfall. Higher values indicate more rainfall	centration			
	concentrated in fewer steps.				
Temporal Concentration	Measures how strongly rain is clustered in time	Temporal con-	\checkmark	\checkmark	
Index (TCI)	around each time-step, selects value for time step	centration			
	around which rainfall is most tightly clustered.				
	A higher TCI means a more tightly concentrated				
	"core" of high rain intensity				
$NRMSE_p$	Quantifies concentration of rainfall near the peak	Temporal Con-	×	×	
	(RMSE from peak, normalised by rainfall total). 0	centration			
	= uniform distribution, 1 = all rainfall in single time				
	step.				
Gini coefficient	Measures inequality of rainfall distribution (higher	Magnitude con-	\checkmark	\checkmark	
	values indicate greater concentration of rainfall in	centration			
	fewer intervals)				
Lorenz asymmetry coeffi-	Quantifies skewness of rainfall intensity distribu-	Magnitude con-	×	×	
cient	tion relative to the mean, distinguishing whether	centration			
	the concentration arises from a few extreme high-				
	intensity bursts or from many moderately intense				
	intervals, even if overall inequality is similar.				





Metric	Meaning	Focus		Robust to:
			Temp res	DMC transformation
% time in LIZ / HIZ	Time spent below / above mean intensity. Indicates	Magnitude con-	×	×
	how long the storm stays intense for.	centration		
% rain in HIZ	Proportion of rainfall in above-average intensity pe-	Magnitude con-	×	×
	riods. More rainfall in HIZ indicates a more concen-	centration		
	trated event.			
Frac. in Q1/Q2/Q3/Q4	% total rainfall in each quarter	Magnitude con-	×	×
		centration		
Temporal (T) kurtosis	Whether rainfall is very concentrated in time around	Temporal con-	✓	\checkmark
	the centre of gravity, or spread out in the tails	centration		
Temporal (T) std	How spread out rainfall is in time around centre of	Temporal con-	✓	✓
	gravity, weighted by heaviness of rain	centration		

 Table C3. Summary of reviewed metrics (Part 3: Intermittency metrics)

Metric	Meaning	Focus		Robust to:
			Temp res	DMC transformation
Event dry ratio	Proportion of event duration spent at 0 mm/hr	Intermittency	×	×
Intermittency fraction	Frequency of wet/dry transitions in the event	Intermittency	×	×





Appendix D: Silhoutte score

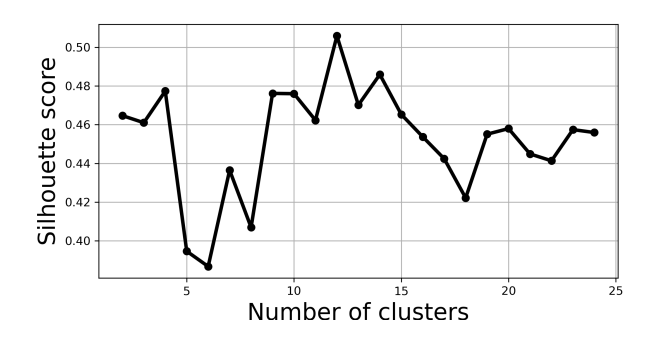


Figure D1. Silhouette scores for different numbers of clusters

Author contributions. Conceptualisation and methodology was by MA and JP, Funding acquisition and supervision by MT and CB. Data curation was by MA, JP and RH. Formal analysis was by MA and RH. Investigation and visualisation was by MA. The original manuscript was written by MA, with review and editing by JP, MT, CB and SB.

Competing interests. The authors declare that they have no conflict of interest.

Acknowledgements. We would like to thank the Water Pollution Committee of The Society of Danish Engineers for allowing us to use their data for this study.

We also extend thanks to Lawrence Jackson for his guidance on the statistical analysis of metrics performed in this study.





References

640

- Morteza Alavinia, Farzin Nasiri Saleh, and Hossain Asadi. Effects of rainfall patterns on runoff and rainfall-induced erosion. *International Journal of Sediment Research*, 34(3):270–278, 2019.
- S Amin, AR Sepaskhah, and B Keshmiripour. Rainfall intensity distribution patterns in climatological conditions of four stations in fars province, iran. *Iranian Journal of Science and Technology*, 24(1):89–98, 2000.
 - Abena O Amponsah, Joseph A Daraio, and Amir A Khan. Implications of climatic variations in temporal precipitation patterns for the development of design storms in newfoundland and labrador. *Canadian Journal of Civil Engineering*, 46(12):1128–1141, 2019.
 - Regimeire Freitas Aquino, Marx Leandro Naves Silva, Diego Antonio França de Freitas, Nilton Curi, and Junior Cesar Avanzi. Soil losses from typic cambisols and red latosol as related to three erosive rainfall patterns. *Revista Brasileira de Ciência do Solo*, 37:213–220, 2013.
 - Molly Asher, Mark Trigg, Steven Boïng, and Cathryn Birch. The sensitivity of urban pluvial flooding to the temporal distribution of rainfall within design storms. *Journal of Flood Risk Management*, 18(3):e70097, 2025.
 - Molly Asher, Jonas Wied Pedersen, Steven Boeing, Cathryn Birch, Mark Trigg, and Elizabeth Kendon. Extreme rainfall and temporal loading in great britain: Analysis of present and future trends using a convection-permitting climate model. *Journal of Hydrology: Regional Studies*, in press. URL https://papers.ssrn.com/sol3/papers.cfm?abstract_id=5239855. Available online ahead of print.
 - M Azli and A Ramachandra Rao. Development of huff curves for peninsular malaysia. Journal of Hydrology, 388(1-2):77-84, 2010.
 - Alvaro José Back and Maria Laura Guimarães Rodrigues. Characterization of temporal rainfall distribution in florianópolis, santa catarina, brazil. *Revista Brasileira de Climatologia*, 28:201–219, 2021.
- Alexis Berne and Witold F Krajewski. Radar for hydrology: Unfulfilled promise or unrecognized potential? *Advances in Water Resources*, 51:357–366, 2013.
 - Nejc Bezak, Mojca Šraj, Simon Rusjan, and Matjaž Mikoš. Impact of the rainfall duration and temporal rainfall distribution defined using the huff curves on the hydraulic flood modelling results. *Geosciences*, 8(2):69, 2018.
 - David M Brommer, Randall S Cerveny, and Robert C Balling Jr. An analysis of intra-event precipitation variability for the united states (1980–2010). *Physical Geography*, 34(6):456–470, 2013.
- Yanpeng Cai, Yueying Yang, Qian Tan, Chao Dai, Zhihua Zhu, and Xiaodong Zhang. Impacts of temporal/spatial rainfall heterogeneities on peak runoff distribution and intensities for an urban river basin of south china. *River*, 3(1):24–37, 2024.
 - Centre for Ecology & Hydrology. *The Flood Estimation Handbook (five volumes). Volume 3: Statistical procedures for flood frequency estimation.* Centre for Ecology & Hydrology, Wallingford, UK, 1999.
- Hoyoung Cha, Jongjin Baik, Jinwook Lee, Wooyoung Na, Sayed M Bateni, and Changhyun Jun. Generation of rainfall scenarios based on rainfall transition probability to determine temporal distribution of independent rainstorms. *Stochastic Environmental Research and Risk Assessment*, pages 1–19, 2024.
 - Zhihe Chen, Lei Yin, Xiaohong Chen, Shuai Wei, and Zhihua Zhu. Research on the characteristics of urban rainstorm pattern in the humid area of southern china: a case study of guangzhou city. *International Journal of Climatology*, 35(14), 2015.
- Aline Franciel de Andrade, Roriz Luciano Machado, Cássia Cristina Rezende, Elizabete Alves Ferreira, Murilo Alceu de Águas, Vladia

 Correchel, and Daniel Fonseca de Carvalho. Precipitation patterns and rainfall erosivity return period under savanna conditions in formosa, goiás, brazil. *Journal of Agricultural Studies*, 8(4):554–569, 2020.





- Abelardo Antônio de Assunção Montenegro, Thais Emanuelle Monteiro dos Santos Souza, Edivan Rodrigues de Souza, and Suzana Maria Gico Lima Montenegro. Temporal dynamics of soil moisture and rainfall erosivity in a tropical volcanic archipelago. *Journal of Hydrology*, 563:737–749, 2018.
- JLMP De Lima and VP Singh. The influence of the pattern of moving rainstorms on overland flow. *Advances in Water Resources*, 25(7): 817–828, 2002.
 - João LMP de Lima, Sílvia CP Carvalho, and M Isabel P de Lima. Rainfall simulator experiments on the importance of when rainfall burst occurs during storm events on runoff and soil loss. *Zeitschrift fur Geomorphologie Supplement*, 57(1):91–109, 2013.
 - DMI. Climate Data DMI Open Data, 2025.
- Domen Dolšak, Nejc Bezak, and Mojca Šraj. Temporal characteristics of rainfall events under three climate types in slovenia. *Journal of Hydrology*, 541:1395–1405, 2016.
 - David Dunkerley. Identifying individual rain events from pluviograph records: a review with analysis of data from an australian dryland site. *Hydrological Processes: An International Journal*, 22(26):5024–5036, 2008.
 - David Dunkerley. The importance of incorporating rain intensity profiles in rainfall simulation studies of infiltration, runoff production, soil erosion, and related landsurface processes. *Journal of Hydrology*, 603:126834, 2021a.
 - David Dunkerley. Intermittency of rainfall at sub-daily timescales: New quantitative indices based on the number, duration, and sequencing of interruptions to rainfall. *Atmospheric Research*, 253:105475, 2021b.
 - David Dunkerley. Huff quartile classification of rainfall intensity profiles ('storm patterns'): A modified approach employing an intensity threshold. *Catena*, 216:106371, 2022.
- Andreas Efstratiadis, Panagiotis Dimas, George Pouliasis, Ioannis Tsoukalas, Panagiotis Kossieris, Vasilis Bellos, Georgia-Konstantina Sakki, Christos Makropoulos, and Spyridon Michas. Revisiting flood hazard assessment practices under a hybrid stochastic simulation framework. *Water*, 14(3):457, 2022.
 - Thomas Einfalt, Karsten Arnbjerg-Nielsen, Claudia Golz, Niels-Einar Jensen, Markus Quirmbach, Guido Vaes, and Baxter Vieux. Towards a roadmap for use of radar rainfall data in urban drainage. *Journal of Hydrology*, 299(3-4):186–202, 2004.
- 690 Linfeng Fan, Peter Lehmann, Chunmiao Zheng, and Dani Or. Rainfall intensity temporal patterns affect shallow landslide triggering and hazard evolution. *Geophysical Research Letters*, 47(1):e2019GL085994, 2020.
 - Francesco Fatone, Bartosz Szeląg, Adam Kiczko, Dariusz Majerek, Monika Majewska, Jakub Drewnowski, and Grzegorz Łagód. Advanced sensitivity analysis of the impact of the temporal distribution and intensity of rainfall on hydrograph parameters in urban catchments. *Hydrology and Earth System Sciences*, 25(10):5493–5516, 2021.
- Hayley J Fowler, Geert Lenderink, Andreas F Prein, Seth Westra, Richard P Allan, Nikolina Ban, Renaud Barbero, Peter Berg, Stephen Blenkinsop, Hong X Do, et al. Anthropogenic intensification of short-duration rainfall extremes. *Nature Reviews Earth & Environment*, 2(2):107–122, 2021.
 - Bernd Frauenfeld and Clint Truman. Variable rainfall intensity effects on runoff and interrill erosion from two coastal plain ultisols in georgia. *Soil Science*, 169(2):143–154, 2004.
- 700 Xiaoran Fu, Jiahong Liu, Chao Mei, Qinghua Luan, Hao Wang, Weiwei Shao, Pingping Sun, and Yunchao Huo. Effect of typhoon rainstorm patterns on the spatio-temporal distribution of non-point source pollution in a coastal urbanized watershed. *Journal of Cleaner Production*, 292:126098, 2021.
 - Guangyao Gao, Yue Liang, Jianbo Liu, David Dunkerley, and Bojie Fu. A modified rusle model to simulate soil erosion under different ecological restoration types in the loess hilly area. *International Soil and Water Conservation Research*, 12(2):258–266, 2024.



720



- Jihui Gao, Mike Kirkby, and Joseph Holden. The effect of interactions between rainfall patterns and land-cover change on flood peaks in upland peatlands. *Journal of Hydrology*, 567:546–559, 2018.
 - Rafael García-Bartual and Ignacio Andrés-Doménech. A two-parameter design storm for mediterranean convective rainfall. *Hydrology and Earth System Sciences*, 21(5):2377–2387, 2017.
- A Garcia-Guzman and E Aranda-Oliver. A stochastic model of dimensionless hyetograph. *Water Resources Research*, 29(7):2363–2370, 1993.
 - Ankit Ghanghas, Ashish Sharma, and Venkatesh Merwade. Unveiling the evolution of extreme rainfall storm structure across space and time in a warming climate. *Earth's Future*, 12(9):e2024EF004675, 2024.
 - L. Gholami, A. Khaledi Darvishan, V. Spalevic, A. Cerdà, and A. Kavian. Effect of storm pattern on soil erosion in damaged rangeland: Field rainfall simulation approach. *Journal of Mountain Science*, 18(3):706–715, 2021. https://doi.org/10.1007/s11629-020-6157-1.
- 715 Ida Bülow Gregersen, Hjalte Jomo Danielsen Sørup, Henrik Madsen, Dan Rosbjerg, Peter Steen Mikkelsen, and Karsten Arnbjerg-Nielsen.

 Assessing future climatic changes of rainfall extremes at small spatio-temporal scales. *Climatic change*, 118:783–797, 2013.
 - R Harshanth, Saha Dauji, and PK Srivastava. Development of site-specific time distribution pattern of rainfall for tarapur, india. *Journal of Earth System Science*, 132(2):77, 2023.
 - Sijing He, Zhaoli Wang, Dagang Wang, Weilin Liao, Xushu Wu, and Chengguang Lai. Spatiotemporal variability of event-based rainstorm: The perspective of rainfall pattern and concentration. *International Journal of Climatology*, 42(12):6258–6276, 2022.
 - Zhengying He, Yu Huang, Yinke Li, and Xingyue Li. Probabilistic fragility assessment of slopes considering uncertainty associated with temporal patterns of rainfall intensity. *Computers and Geotechnics*, 173:106534, 2024.
 - Suresh Hettiarachchi, Conrad Wasko, and Ashish Sharma. Increase in flood risk resulting from climate change in a developed urban watershed—the role of storm temporal patterns. *Hydrology and Earth System Sciences*, 22(3):2041–2056, 2018.
- WW Horner and SW Jens. Surface runoff determination from rainfall without using coefficients. *Transactions of the American Society of Civil Engineers*, 107(1):1039–1075, 1942.
 - Shanshan Hu, Fan Feng, Wenbin Liu, and Dunxian She. Changes in temporal inequality and persistence of precipitation over china during the period 1961–2013. *Hydrology Research*, 49(4):1283–1291, 2018.
 - Floyd A Huff. Time distribution of rainfall in heavy storms. Water resources research, 3(4):1007-1019, 1967.
- 730 Anil K Jain, M Narasimha Murty, and Patrick J Flynn. Data clustering: a review. ACM computing surveys (CSUR), 31(3):264–323, 1999.
 - Dong Jin Jeon, Seo Jin Ki, Sang-Soo Baek, YoonKyung Cha, Kyung Hwa Cho, Kwang-Sik Yoon, Hyun Suk Shin, and Joon Ha Kim. Assessing the efficiency of aggregate low impact development (lid) at a small urbanized sub-catchment under different storm scenarios. Desalination and Water Treatment, 86:1–8, 2017.
 - Changhyun Jun, Xiaosheng Qin, Mengzhu Chen, and Hyungjoon Seo. Investigating event-based temporal patterns of design rainfall in a tropical region. *Hydrological Sciences Journal*, 66(13):1986–1996, 2021.
 - Shih-Chieh Kao and Rao S Govindaraju. Trivariate statistical analysis of extreme rainfall events via the plackett family of copulas. *Water Resources Research*, 44(2), 2008.
 - Clint J Keifer and Henry Hsien Chu. Synthetic storm pattern for drainage design. *Journal of the hydraulics division*, 83(4):1332–1, 1957. Maurice G Kendall. A new measure of rank correlation. *Biometrika*, 30(1-2):81–93, 1938.
- Nobuaki Kimura, Akira Tai, Shen Chiang, Hsiao-Ping Wei, Yuan-Fong Su, Chao-Tzuen Cheng, and Akio Kitoh. Hydrological flood simulation using a design hyetograph created from extreme weather data of a high-resolution atmospheric general circulation model. *Water*, 6 (2):345–366, 2014.



755

765



- K Klamkowski, W Treder, and A Tryngiel-Gać. The effect of rainfall intensity and floor management practices on changes in soil water status in an apple orchard. pages 539–544, 2012.
- James O Knighton and M Todd Walter. Critical rainfall statistics for predicting watershed flood responses: rethinking the design storm concept. *Hydrological processes*, 30(21):3788–3803, 2016.
 - NT Kottegoda and AHM Kassim. Classification of storm profiles using crossing properties. Journal of Hydrology, 127(1-4):37-53, 1991.
 - Geert Lenderink and Erik Van Meijgaard. Unexpected rise in extreme precipitation caused by a shift in rain type? *Nature Geoscience*, 2(6): 373–373, 2009.
- Runze Li, Clement Guilloteau, Pierre-Emmanuel Kirstetter, and Efi Foufoula-Georgiou. How well does the imerg satellite precipitation product capture the timing of precipitation events? *Journal of Hydrology*, 620:129563, 2023.
 - Ting Li, Gyuwon Lee, and Gwangseob Kim. Case study of urban flood inundation—impact of temporal variability in rainfall events. *Water*, 13(23):3438, 2021.
 - Yue Liang, Guangyao Gao, Jianbo Liu, David Dunkerley, and Bojie Fu. Runoff and soil loss responses of restoration vegetation under natural rainfall patterns in the loss plateau of china: The role of rainfall intensity fluctuation. *Catena*, 225:107013, 2023.
 - Jianbo Liu, Yue Liang, Guangyao Gao, David Dunkerley, and Bojie Fu. Quantifying the effects of rainfall intensity fluctuation on runoff and soil loss: From indicators to models. *Journal of Hydrology*, 607:127494, 2022.
 - Kaihao Long, Dagang Wang, Guiling Wang, Jinxin Zhu, Shuo Wang, and Shuishi Xie. Higher temperature enhances spatiotemporal concentration of rainfall. *Journal of Hydrometeorology*, 22(12):3159–3169, 2021.
- Athanasios Loukas and Michael C Quick. Spatial and temporal distribution of storm precipitation in southwestern british columbia. *Journal of hydrology*, 174(1-2):37–56, 1996.
 - Melanie Loveridge, Mark Babister, and M Retallick. Australian rainfall and runoff revision project 3: Temporal patterns of rainfall. *Engineers Australia, Barton*, 2015.
 - Wei Lu and Xiaosheng Qin. Integrated framework for assessing climate change impact on extreme rainfall and the urban drainage system. *Hydrology Research*, 51(1):77–89, 2020.
 - Xiangyu Lu, Tianfu Wen, Linus Zhang, and Qi Zhang. Impact of spatiotemporal rainfall distribution and underlying surface changes on flood processes in meijiang river basin, china. *Water*, 17(4):466, 2025.
 - Spyros Makridakis and Michèle Hibon. Evaluating accuracy (or error) measures, 1995.
 - David Moher, Alessandro Liberati, Jennifer Tetzlaff, Douglas G Altman, Prisma Group, et al. Preferred reporting items for systematic reviews and meta-analyses: the prisma statement. *International journal of surgery*, 8(5):336–341, 2010.
 - Isabel Molina-Sanchis, Roberto Lázaro, Eva Arnau-Rosalén, and Adolfo Calvo-Cases. Rainfall timing and runoff: The influence of the criterion for rain event separation. *Journal of Hydrology and Hydromechanics*, 64(3):226, 2016.
 - Thomas Müller, Manfred Schütze, and András Bárdossy. Temporal asymmetry in precipitation time series and its influence on flow simulations in combined sewer systems. *Advances in Water Resources*, 107:56–64, 2017.
- 775 Werner Nel. Intra-storm attributes of extreme storm events in the drakensberg, south africa. Physical Geography, 28(2):158–169, 2007.
 - C WW Ng, B Wang, and Yeou-Koung Tung. Three-dimensional numerical investigations of groundwater responses in an unsaturated slope subjected to various rainfall patterns. *Canadian Geotechnical Journal*, 38(5):1049–1062, 2001.
 - Dinh Ty Nguyen and Shien-Tsung Chen. Generating continuous rainfall time series with high temporal resolution by using a stochastic rainfall generator with a copula and modified huff rainfall curves. *Water*, 14(13):2123, 2022.



790



- 780 Byunghwa Oh, JongChun Kim, and Seokhwan Hwang. Influence of rainfall patterns on rainfall–runoff processes: Indices for the quantification of temporal distribution of rainfall. *Water* (20734441), 16(20), 2024.
 - John E Oliver. Monthly precipitation distribution: a comparative index. The Professional Geographer, 32(3):300-309, 1980.
 - Fabio Oriani, Raj Mehrotra, Grégoire Mariethoz, Julien Straubhaar, Ashish Sharma, and Philippe Renard. Simulating rainfall time-series: how to account for statistical variability at multiple scales? *Stochastic Environmental Research and Risk Assessment*, 32:321–340, 2018.
- 785 Matteo Pampaloni, Alvaro Sordo-Ward, Paola Bianucci, Ivan Gabriel-Martin, Enrica Caporali, and Luis Garrote. A stochastic procedure for temporal disaggregation of daily rainfall data in suds design. *Water*, 13(4):403, 2021.
 - AJ Parsons and PM Stone. Effects of intra-storm variations in rainfall intensity on interrill runoff and erosion. Catena, 67(1):68–78, 2006.
 - Antonio G Pinheiro, Thais EM dos S Souza, Suzana MGL Montenegro, Abelardo A de A Montenegro, and Sérgio Guerra. Rainfall pattern and erosion potential in the physiographic regions of the state of pernambuco, brazil. *Revista Brasileira de Engenharia Agrícola e Ambiental*, 22:849–853, 2018.
 - Ina Pohle, Michael Niebisch, Hannes Müller, Sabine Schümberg, Tingting Zha, Thomas Maurer, and Christoph Hinz. Coupling poisson rectangular pulse and multiplicative microcanonical random cascade models to generate sub-daily precipitation timeseries. *Journal of Hydrology*, 562:50–70, 2018.
 - Pedro J Restrepo-Posada and Peter S Eagleson. Identification of independent rainstorms. Journal of Hydrology, 55(1-4):303-319, 1982.
- Diego Rivera, José Luis Arumí, and Mario Lillo-Saavedredra. Spatio-temporal patterns in soil water content time series: Influence of the time series length and precipitation events. page 1, 2012.
 - Mathias JM Römkens, K Helming, and SN Prasad. Soil erosion under different rainfall intensities, surface roughness, and soil water regimes. *Catena*, 46(2-3):103–123, 2002.
- J Rousseeuw, Peter. A graphical aid to the interpretation and validation of cluster analysis. *Journal of Computational and Applied Mathe-*800 *matics*, 20:53–65, 1987.
 - Leonard Schiff. Classes and pattern of rainfall with reference to surface-runoff. *Eos, Transactions American Geophysical Union*, 24(2): 438–452, 1943.
 - Wolfgang Schilling. Rainfall data for urban hydrology: what do we need? Atmospheric Research, 27(1-3):5-21, 1991.
- José Roberto Vicencio Serna and Cayo Leonidas Ramos Taipe. Determination of storm profiles in the central andes of peru. In *E-proceedings* of the 38th IAHR World Congress, 2019.
 - OG Terranova and P Iaquinta. Temporal properties of rainfall events in calabria (southern italy). *Natural hazards and earth system sciences*, 11(3):751–757, 2011.
 - Emma Dybro Thomassen, Karsten Arnbjerg-Nielsen, Hjalte Jomo Danielsen Sørup, Peter L. Langen, Jonas Olsson, Rasmus Anker Pedersen, and Ole Bøssing Christensen. Spatial and temporal characteristics of extreme rainfall: Added benefits with sub-kilometre-resolution climate model simulations? *Quarterly Journal of the Royal Meteorological Society*, 149:1913–1931, 2023.
 - Jiyang Tian, Jia Liu, Denghua Yan, Chuanzhe Li, and Fuliang Yu. Numerical rainfall simulation with different spatial and temporal evenness by using a wrf multiphysics ensemble. *Natural Hazards and Earth System Sciences*, 17(4):563–579, 2017.
 - Francesca Todisco. The internal structure of erosive and non-erosive storm events for interpretation of erosive processes and rainfall simulation. *Journal of Hydrology*, 519:3651–3663, 2014.
- Kevin E Trenberth, Aiguo Dai, Roy M Rasmussen, and David B Parsons. The changing character of precipitation. *Bulletin of the American Meteorological Society*, 84(9):1205–1218, 2003.





- M Tsubo, S Walker, and M Hensley. Quantifying risk for water harvesting under semi-arid conditions: Part i. rainfall intensity generation. *Agricultural Water Management*, 76(2):77–93, 2005.
- Gabriela Urgilés, Rolando Célleri, Jörg Bendix, and Johanna Orellana-Alvear. Identification of spatio-temporal patterns in extreme rainfall events in the tropical andes: A clustering analysis approach. *Meteorological Applications*, 31(5):e70005, 2024.
 - K Vantas, E Sidiropoulos, and M Vafeiadis. Optimal temporal distribution curves for the classification of heavy precipitation using hierarchical clustering on principal components. 2019.
 - Carlos Varga, James E Ball, and Mark Babister. A hydroinformatic approach to development of design temporal patterns of rainfall. *IAHS-AISH Publication*, 2009.
- Roberto Villalobos Herrera, Stephen Blenkinsop, Selma B Guerreiro, Murray Dale, Duncan Faulkner, and Hayley J Fowler. Towards new design rainfall profiles for the United Kingdom. *Journal of Flood Risk Management*, page e12958, 2023.
 - Johan B Visser, Conrad Wasko, Ashish Sharma, and Rory Nathan. Changing storm temporal patterns with increasing temperatures across australia. *Journal of Climate*, 36(18):6247–6259, 2023.
- Fan Wang. Temporal pattern analysis of local rainstorm events in china during the flood season based on time series clustering. *Water*, 12 (3):725, 2020.
 - Guoqiang Wang, Wenchao Sun, Baolin Xue, Anthony Kiem, et al. Stratification response of soil water content during rainfall events under different rainfall patterns. *Hydrological processes*, 32(20), 2018.
 - Hao Wang, Rui Chen, Anthony Kwan Leung, and Ankit Garg. Hydrological responses to early-peak rainfall in unsaturated rooted soils. *Heliyon*, 9(5), 2023.
- Wenting Wang, Shuiqing Yin, Yun Xie, Baoyuan Liu, and Yingna Liu. Effects of four storm patterns on soil loss from five soils under natural rainfall. *Catena*, 141:56–65, 2016.
 - Katarzyna Wartalska and Andrzej Kotowski. Model hyetographs of short-term rainfall for wrocław in the perspective of 2050. *Atmosphere*, 11(6):663, 2020.
- Katarzyna Wartalska, Bartosz Kaźmierczak, Monika Nowakowska, and Andrzej Kotowski. Analysis of hyetographs for drainage system modeling. *Water*, 12(1):149, 2020.
 - Conrad Wasko and Ashish Sharma. Steeper temporal distribution of rain intensity at higher temperatures within australian storms. *Nature Geoscience*, 8(7):527–529, 2015.
 - Tara Williams-Sether. Empirical, dimensionless, cumulative-rainfall hyetographs developed from 1959-86 storm data for selected small watersheds in Texas. Number 2004. US Geological Survey, 2004.
- Jie Yang, Ying Xiang, Xiazhen Xu, and Jiali Sun. Design hyetograph for short-duration rainstorm in jiangsu. Atmosphere, 13(6):899, 2022.
 Junhua Yang, Keqin Duan, Jinkui Wu, Xiang Qin, Peihong Shi, Huancai Liu, Xiaolong Xie, Xiao Zhang, and Jianyong Sun. Effect of data assimilation using wrf-3dvar for heavy rain prediction on the northeastern edge of the tibetan plateau. Advances in Meteorology, 2015(1): 294589, 2015.
- Po Yang, Zexing Xu, Xufeng Yan, and Xiekang Wang. Establishing a rainfall dual-threshold for flash flood early warning considering rainfall patterns in mountainous catchment, china. *Natural Hazards*, 120(7):6657–6684, 2024.
 - In-Kwon Yeo and Richard A Johnson. A new family of power transformations to improve normality or symmetry. *Biometrika*, 87(4): 954–959, 2000.
 - Shui-qing Yin, Yun Xie, Mark A Nearing, Wen-li Guo, and Zheng-yuan Zhu. Intra-storm temporal patterns of rainfall in china using huff curves. *Transactions of the ASABE*, 59(6):1619–1632, 2016.





- 855 XC Zhang, LD Norton, and M Hickman. Rain pattern and soil moisture content effects on atrazine and metolachlor losses in runoff. Technical report, Wiley Online Library, 1997.
 - Yihui Zhang, Kang Liang, and Changming Liu. Time distribution pattern and spatial heterogeneity of hourly scale event-based extreme precipitation in china. *Journal of Hydrology*, 622:129712, 2023.
- Binru Zhao, Roberto J Marin, Wen Luo, Zhaoyuan Yu, and Linwang Yuan. Rainfall thresholds for shallow landslides considering rainfall temporal patterns. *Bulletin of Engineering Geology and the Environment*, 84(3):1–13, 2025.